



Master's Thesis in Economics

Alexander Michael Peytz

Dynamic Portfolio Choice with Fixed and Proportional Transaction Costs and Correlated Return Structures

A Dynamic Programming Approach

Advisor: Bertel Schjerning

Submitted: December 20, 2024

Keystrokes: 120.778 (50, 32 normal pages)

Dynamic Portfolio Choice with Fixed and Proportional Transaction Costs and Correlated Return Structures*

Master's Thesis
Alexander Michael Peytz[†]

December 20, 2024

Abstract

This thesis solves dynamic portfolio allocation problems with fixed and proportional transaction costs and correlated return structures. The models are solved using a combination of dynamic programming (DP), numerical methods and machine learning techniques, using the most recent advances on solving dynamic portfolio choice problems with proportional transaction costs. This thesis contributes to the existing literature in a multitude of ways. Firstly, I present a novel approach to the fixed costs problem based on the state of the art framework for proportional costs. This leverages the geometric shape of the No-Trade Region (NTR) which occurs due to the transaction costs. Secondly, this thesis is the first, to my knowledge, to solve dynamic portfolio choice problems with fixed costs, correlated returns and more than two risky assets, providing insight into the shape of the NTR with fixed costs. Thirdly, I present findings on the combination of fixed and proportional costs and the resulting NTR shape in relation to the two costs. Lastly, I present an approach to solving new transaction costs structures, not yet considered, and how to adapt my computational approach to these, paving the way for future research in this area.

*I thank my supervisor Bertel Schjerning for his patient guidance and support. I also thank my partner for helpful advice and encouragement.

[†]Department of Economics, University of Copenhagen. E-mail: kqw203@alumni.ku.dk.

Table of Contents

1	Introduction	6
2	Literature review	7
3	The Dynamic Portfolio Choice Setting	9
3.1	Asset and goods market	9
3.2	Asset dynamics	10
3.3	Transaction costs and portfolio reallocation	10
3.4	Investor preferences and problem	11
3.5	Intertemporal portfolio choice without transaction costs	12
3.6	The general class of dynamic portfolio choice with transaction costs and intertemporal consumption	13
3.7	No Trade Region (NTR)	16
3.8	Base problem: Portfolio choice with proportional costs and consumption .	17
3.9	Portfolio choice with fixed costs	17
3.10	Portfolio choice with fixed and proportional costs	18
4	Numerical implementation details	19
4.1	Numerical integration	19
4.1.1	Gauss-Hermite quadrature	19
4.1.2	Monte Carlo integration (MC)	22
4.1.3	Quasi-Monte Carlo integration (QMC)	23
4.1.4	Randomized Quasi-Monte carlo integration (RQMC)	25
4.1.5	Choice of numerical integration technique	25
4.2	Value function approximation	26
4.2.1	Gaussian process regressions (GPR)	26
4.3	Approximating the No trade region	28
4.3.1	Strategic point sampling	30
4.3.2	Utilizing the NTR approximation for δ bounds	32
4.3.3	Multiple Gaussian Process Regressions	32
4.4	Final solution algorithms	33
4.5	Computational stack and implementation	34
4.5.1	Optimization details	35
5	Results	35
5.1	Parameters and Model Setup	36
5.2	Dynamic Portfolio Choice without consumption	36
5.2.1	Verifying the geometric shape of the No-trade Region	38

5.2.2	Investigating the No-Trade Region	39
5.2.3	Increasing the dimensionality of the model	40
5.3	Dynamic Portfolio Choice with consumption	41
5.3.1	Increasing the dimensionality of the model further	43
5.4	Dynamic Portfolio Choice with fixed costs	44
5.4.1	Generating a new solution algorithm for the fixed cost case	44
5.4.2	Constructing a new sampling scheme and approximation method for the NTR	45
5.4.3	Fixed costs No-Trade Region without correlation	48
5.5	Dynamic Portfolio Choice with fixed costs and correlation	49
5.6	Adjusting the algorithm to new cost structures or assets	52
5.7	Portfolio simulations	52
5.7.1	Portfolio simulations with fixed costs	53
5.8	Dynamic Portfolio Choice with fixed and proportional costs	55
6	Discussion	58
6.1	Applicability of the model	58
6.2	Scalability of the model	59
6.3	Competing implementation methods	60
6.4	Avenues of Future Research	60
7	Conclusion	61
Appendices		65

List of Figures

3.1	Example No Trade Region with two risky assets.	16
4.1	Comparison of sample generation for Monte Carlo and Quasi-Monte Carlo	24
4.2	Comparison of sample generation for Monte Carlo and Quasi-Monte Carlo with increased dimensionality	24
4.3	Schematic of the No-Trade Region	29
4.4	The designed sampling strategy for state space coverage.	31
5.1	Comparison of No Trade Regions with proportional costs.	37
5.2	Verifying the assumptions of the NTR in two dimensions.	38
5.3	No Trade Region for Schober Parameters over Time.	39
5.4	No Trade Region for the i.i.d Parameters with different values of τ .	40
5.5	Comparison of No Trade Regions with three risky assets.	40
5.6	Comparison of No Trade Regions over time with consumption.	41
5.7	No trade regions with consumption in multiple dimensions, singular time period	42
5.8	No trade regions with consumption in multiple dimensions entire horizon	43
5.9	No trade regions for Shober parameters with consumption, four assets projected to three dimensions.	44
5.10	Grid solution to the i.i.d case with fixed costs, two assets in period $T - 1$.	46
5.11	Two dimensional approximation algorithm for the fixed cost NTR with no correlation.	47
5.12	Sampling strategy for the fixed cost NTR, with no consumption or correlation.	47
5.13	Fixed cost No-Trade Regions with i.i.d assets.	48
5.14	Grid solution to the high correlation case with fixed costs and two assets in period $T - 1$.	49
5.15	NTR for two assets with fixed costs and high correlation parameters.	51
5.16	Three asset No-Trade Regions with fixed costs and correlation	51
5.17	Simulated returns for the two assets over time.	53
5.18	Simulated variables over time for the fixed cost case.	54
5.19	Grid solution for two assets with fixed and proportional costs and Schober parameters.	55
5.20	Schematic of the complex shaped NTR with both fixed and proportional costs.	57
A.1	Uniform grid sampling strategy	65
A.2	Naive random sampling strategy	65
C.1	Fitting shceme for the 3D sphere NTR	67

List of Tables

1	Parameters for portfolio models	36
---	---	----

Abbreviations

DP	Dynamic Programming
GP	Gaussian process
GPR	Gaussian process regression
LDS	Low-Discrepancy Sequences
MC	Monte Carlo
MPT	Modern Portfolio Theory
NTR	No-Trade Region
PML	Probabilistic Machine Learning
QMC	Quasi-Monte Carlo
RQMC	Randomized Quasi-Monte Carlo

1 Introduction

Dynamic portfolio choice problems consider the optimal portfolio construction over time. These have a general solution in the absence of market frictions. When frictions are introduced, the problem is more realistic, as investors face costs when trading assets. However, this increased realism comes at a tradeoff of increased complexity, as the optimal portfolio construction is no longer trivial to find. Investors typically face two types of costs when trading assets: fixed costs and proportional costs.

Proportional costs have been studied extensively in the literature, and optimal portfolio construction is well understood. Fixed costs, on the other hand, have been less studied and the optimal portfolio construction is not as well defined, especially so, when the asset returns are correlated or the number of risky assets is greater than two.

For dynamic portfolio choice models with proportional costs, Dynamic Programming (DP) schemes have been implemented to solve these problems numerically, but the computational complexity of these schemes suffer from the curse of dimensionality in a multitude of ways using multiple grid-based methods. In this regard, the work of (Gaegauf, Scheidegger and Trojani 2023) is of particular interest to me, as they develop a computational framework which reduces the need for grid-based methods. While much work has been put into developing a computational framework which reduces the need for grid-based methods, this has not been applied to a broader set of portfolio choice models, and the scope of applicability of these methods has not been fully explored.

I therefore extend the framework of (Gaegauf, Scheidegger and Trojani 2023) to include fixed costs with correlated asset returns. I do so to broaden the scope of models which can be solved and to provide clarity on this class of dynamic portfolio choice problems.

I display the impact of fixed costs on the optimal portfolio construction, and how this differs from proportional costs. In doing so, I provide a novel approach to solving the fixed costs problem, based on the state of the art framework for proportional costs. My approach leverages the geometric properties of the No-Trade Region (NTR), stemming from the trade frictions. This alleviates the computational burden of the problem. However, I find that the fixed costs problem is more complex to solve than the proportional costs problem.

I find that the NTR under fixed costs schemes, is circular when asset returns are uncorrelated and elliptical when they are correlated. This is in contrast to the NTR under proportional costs, which is a convex polytope.

I furthermore solve the fixed cost problem for three risky assets, which has not been done in the literature to my knowledge, and show that the resulting geometric shape of the NTR, is the direct higher order generalization of the two risky assets case.

In addition to this I provide an intuitive approach, to solving new cost structures, not considered in this thesis, and how to adapt the computational approach to these. This

paves the way for future research in this area.

This thesis is structured as follows. In Section 2, I review the literature on dynamic portfolio choice problems with transaction costs, so my contributions can be placed in context of the existing literature. In Section 3, I cover the theoretical framework of the model, relevant assumptions and the economic intuition behind the model. I also present the general class of problems which this thesis aims to solve. In Section 4, I present the computational framework, and how it is implemented for the proportional cost case. In Section 5, I present the results of the model. I first cover the results of the proportional cost case and then the fixed cost case. For the latter I present how the computational framework is extended to include fixed costs, and how the results differ from the proportional cost case. I also combine the two costs and present the results of this. In Section 6, I discuss the applicability of the model, the scalability of the proposed solution framework and future research avenues. I lastly conclude on the findings of this thesis.

2 Literature review

The purpose of this section is to review relevant literature to help understand the contributions made in this thesis, and their relation to the existing literature. This review covers dynamic portfolio choice problems, the introduction of transaction costs, and most notable contributions to the field.

Modern theory on portfolio choice can be traced back to the mean-variance framework of Harry Markowitz, who constructed and solved the static and single period, portfolio optimization problem, (Markowitz 1952).

This covers the mean-variance framework which is the foundation of Modern Portfolio Theory (MPT), suggesting investors should allocate wealth in order to maximize expected return, while minimizing exposure to risk. Following this, the mean-variance framework has since been extended, most notably by Robert Merton, who introduced a solution to the intertemporal portfolio choice problem in frictionless markets, (Merton 1969). This solution is known as the Merton point in the asset allocation space or the Merton portfolio. Merton's closed form solution suggests optimal asset allocations based on the asset return dynamics (mean-variance), and the risk aversion of the investor (preferences). Later, an optimal consumption rule was found aswell (Merton 1971).

Multiple extensions have been made to the dynamic portfolio choice problem, such as the introduction of transaction costs, adding realistic frictions to the problem, since trading assets incurs costs in the real world, and markets are not frictionless. Most of the literature find that transaction costs create a region in the asset space, where it is sub-optimal to trade, known as the No-Trade Region (NTR).

The literature on proportional costs in the dynamic portfolio choice problem is vast, whereas the fixed costs problem is less explored. (Morton and Pliska 1995) analyse the problem with a fixed cost, relative to the investors wealth, and solve the problem numerically for two correlated risky assets. They find a NTR which is similar to an ellipse but with vertices. They conclude that the NTR is an ellipse. (Liu 2004) solves the problem for uncorrelated assets with proportional and fixed costs and consumption. With fixed costs, No-Trade bounds are found for one risky asset in the shape of a conic. Results differ from (Morton and Pliska 1995), as the fixed cost NTR is not an ellipse but has corners. They conjecture this to be the case for correlated assets as well but skewed. For proportional and fixed costs, multiple target portfolios are found inside the NTR, one for each corner, and the shape of the NTR is square. (Altarovici, Muhle-Karbe and Soner 2015) solve the dynamic problem for two uncorrelated risky assets with fixed costs. They find that the NTR is a slightly angled ellipsoid, using a differential equation approach. (Dybvig and Pezzo 2020) provide a comprehensive review of different transaction costs, and the implications of these on the optimal portfolio choice problem, however the setting is static. They find that the NTR from fixed costs with no correlation is circular, similar to the results of (Morton and Pliska 1995). From this, the exact shape of the fixed cost NTR is not entirely clear. Most find an ellipsoid, but the skewness, connection to the correlation of the asset returns, and whether the NTR has corners or not, is not entirely clear. Furthermore, solutions in the literature are limited to two risky assets, and the solution methods for the dynamic setting has not followed the same advances as the proportional costs problem.

(Zabel 1973; Constantinides 1976; Constantinides 1986) find that for multiple preference types, under proportional transaction costs, the investors decision depends on the remaining life span, wealth and current allocation. Transaction costs entail an NTR, where the optimal reallocation decision for portfolios inside, is to do nothing, and for portfolios outside this region, the optimal decision is to trade towards the boundary of the NTR. This is a shift from Mertons framework, where constant trading toward the Merton allocation, which is the optimal allocation in the absence of transaction costs, is optimal. Thus, transaction costs restrain investors from acting optimally in the classical sense. Numerical examples only cover the case of one risky asset with restrictions on the decision space and results remain qualitative or approximate.

Notably, (Davis and Norman 1990) derive explicit solutions for the case of a single risky asset. They similarly find that proportional transaction costs lead to a NTR around the Merton point and provide a solution algorithm for the stochastic control problem.

(Akian, Menaldi and Sulem 1996) use a Bellman equation in the N-dimensional asset space, and provide further insight to the properties of the NTR, however the problem is only solved for the case of two risky assets with one risk free asset. Further analysis of this has been conducted extensively, e.g see (Shreve and Soner 1994; Oksendal and

Sulem 2002; Janeček and Shreve 2004), however the asset space is still constrained or solutions remain asymptotic. (Muthuraman and Kumar 2006; Muthuraman and Kumar 2008) tackle a three risky asset space and provide a numerical solution to the problem, using a finite differences method.

The paper by (Cai, Judd and Xu 2013), which is central to this thesis, considers a more general setting with multiple risky assets and a risk-free asset and provide a solution algorithm based on DP, numerical integration and polynomial approximation. They solve the dynamic problem for up to six risky assets, and later introduce and solve the problem with novelties, such as stochastic asset parameters or an option on a underlying asset in the portfolio (Cai, Judd and Xu 2020). This work only considers proportional transaction costs and relies on a super computer to solve the problem.

The curse of dimensionality, which haunts the prior methods applied, is somewhat tackled by the use of adaptive sparse grid methods and sparse quadrature rules by (Schober, Valentin and Pflüger 2022). However, results require the use of super computers. (Gaegau, Scheidegger and Trojani 2023) further reduce the computational burden by using a Gaussian process regression (GPR), to approximate value functions and provide a problem specific point-sampling strategy to reduce the number of points in the state space needed to approximate the NTR. Increasing the dimensions of the asset space does still increase the dimensionality of the problem and the computational burden, however this is at a much lower extent than previous methods. This is the most recent computational advance currently in the field, and is basis for the computational framework in this thesis.

3 The Dynamic Portfolio Choice Setting

This section covers the theoretical setting and components of the dynamic portfolio choice problem with transaction costs. This section leans heavily on (Cai, Judd and Xu 2020) and (Gaegau, Scheidegger and Trojani 2023), bridging both models to create a comprehensive framework for the dynamic portfolio choice problem with transaction costs. I first cover the individual components of the model, and then present the general class of dynamic portfolio choice problems with transaction costs. The baseline model with proportional costs is covered and extended to include fixed costs.

3.1 Asset and goods market

I consider a financial market with D risky assets and one risk-free asset, making the asset space $1 + D$ dimensions. The risk-free asset, such as a bond or a bank deposit, yields a constant gross return $R_f = e^{r\Delta t}$, where r is the annual interest rate and $\Delta t = \frac{T}{N}$ is the length of one investment period. The risk-free asset is assumed to be liquid and can be traded without transaction costs. The investor has wealth W_t at time t , which is

allocated between the risk-free asset, the risky assets and consumption. For each time period all wealth must be allocated to either of these.

The D risky assets can be considered as listed stocks, subject to proportional transaction costs. For each reallocation of wealth in a risky asset, a transaction cost of $\tau \in [0, 1]$ is incurred as a percentage of the traded amount. The stochastic one-period gross-return vector of the risky assets is denoted as $\mathbf{R} = (R_1, R_2, \dots, R_D)^\top$, and the corresponding net-return vector is $\mathbf{r} = (r_1, r_2, \dots, r_D)^\top$.

In the goods market, there is a single non-durable consumption good, C , which is consumed at each time point t . The fraction of wealth allocated to consumption at time t is denoted c_t , the fraction allocated to risky assets is $\mathbf{x}_t = (x_{1,t}, x_{2,t}, \dots, x_{k,D})^\top$, and the fraction allocated to the risk-free asset is denoted¹ b_t . I assume that no shorting of assets, or borrowing is allowed, thus the variables are constrained by $\sum_{i=1}^D x_{i,t} + b_t \leq 1$ and $\mathbf{x}_t \in [0, 1]^D$ and $b_t \in [0, 1]$, whereas actual amounts denoted in currency exists in \mathbb{R}^+ .

3.2 Asset dynamics

I follow Cai, Judd and Xu (2013) for the asset dynamics. The total composition of risky assets is assumed to follow a multivariate log-normal distribution:

$$\log(\mathbf{R}) \sim \mathcal{N}\left(\left(\mu - \frac{\sigma^2}{2}\right)\Delta t, (\boldsymbol{\Lambda}\boldsymbol{\Sigma}\boldsymbol{\Lambda})\Delta t\right), \quad (1)$$

where μ is the drift vector, σ^2 is a column vector of the variance σ_i^2 , $\boldsymbol{\Sigma}$ is the correlation matrix, and $\boldsymbol{\Lambda} = \text{diag}(\sigma_1, \sigma_2, \dots, \sigma_k)$ is the diagonal matrix of volatilities. Following Cai, Judd and Xu (2013) I utilize the Cholesky decomposition of the correlation matrix, $\boldsymbol{\Sigma} = \mathbf{L}\mathbf{L}^\top$, where $\mathbf{L} = (L_{i,j})_{k \times k}$ is a lower triangular matrix. Hence, for each risky asset i , the log-return is:

$$\log(R_i) = \left(\mu_i - \frac{\sigma_i^2}{2}\right)\Delta t + \sigma_i\sqrt{\Delta t}\sum_{j=1}^i L_{i,j}z_j, \quad (2)$$

where z_i are independent, standard normal random variables.

3.3 Transaction costs and portfolio reallocation

Rebalancing is subject to proportional transaction costs $\tau \in [0, 1]$, which are paid based on the amount bought or sold of each risky asset. Reallocation decisions are made just before $t_j + \Delta t$, such that \mathbf{x}_t is the portfolio of risky assets right before reallocation, and before portfolio returns are incurred, this is akin to trading decisions being made before the market opens. $\delta_{i,t}$ denotes the change in portfolio allocation of asset i , and $\delta_{i,t}W_t$ is

¹This notation stems from earlier literature, where the risk free asset is a risk free bond.

thus the currency amount traded in asset i . Hence $\delta_{i,t} > 0$ implies buying asset i , and $\delta_{i,t} < 0$ implies selling asset i . Proportional transaction costs imply that the cost function associated with rebalancing is:

$$\psi(\delta_{i,t} W_t) = \tau |\delta_{i,t} W_t| \quad (3)$$

I decompose the decision variable $\delta_{i,t}$, representing the fraction of wealth used to trade risky asset i , into buying ($\delta_{i,t}^+$) and selling ($\delta_{i,t}^-$) components to ensure tractability²:

$$\delta_{i,t} = \delta_{i,t}^+ - \delta_{i,t}^-, \quad \delta_{i,t}^+, \delta_{i,t}^- \geq 0.$$

The total transaction cost is then given by $\tau \sum_{i=1}^k (\delta_{i,t}^+ + \delta_{i,t}^-) W_t$. The transaction cost function is therefore a function of each trading direction:

$$\psi(\delta_{i,t}^+, \delta_{i,t}^-, W_t) = \tau (\delta_{i,t}^+ + \delta_{i,t}^-) W_t \quad (4)$$

Following the reallocation, the remaining wealth is allocated between the risk-free asset and consumption. Notation of rebalancing is henceforth simplified using vectors to $\boldsymbol{\delta}_t = \boldsymbol{\delta}_t^+ - \boldsymbol{\delta}_t^-$ with $\boldsymbol{\delta}_t^+ = (\delta_{1,t}^+, \delta_{2,t}^+, \dots, \delta_{D,t}^+)$ and $\boldsymbol{\delta}_t^- = (\delta_{1,t}^-, \delta_{2,t}^-, \dots, \delta_{D,t}^-)$. $\boldsymbol{\delta}_t$ is the *net change* in the risky positions, and $\boldsymbol{\delta}_t^+ + \boldsymbol{\delta}_t^-$ is the *total trading volume* in the risky positions. Total trading volume is linked to the transaction costs, and the net change is linked to the portfolio allocation.

3.4 Investor preferences and problem

The investor operates over a finite horizon of T years, during which the aim is to maximize expected utility. Following Cai, Judd and Xu (2013), the investment horizon is discretized into N equally spaced periods, each with a duration of $\Delta t = \frac{T}{N}$. Hence this is a discrete time model, which converges to the continuous time model as $\Delta t \rightarrow 0$. At each time point t_j , for $j = 0, 1, \dots, N$, where $t_0 = 0$ and $t_N = T$, the investor has the opportunity to adjust the portfolio allocations right before $t_j + \Delta t$. Reallocation is costly, and the investor is subject to proportional transaction costs. If consumption is included the investor may also choose to consume a non-durable good at each time point.

For notational simplicity, I now use t to denote these time points unless specifically referring to t_j . The investor's preferences are isoelastic, i.e I use a constant relative risk

²Gaegau, Scheidegger and Trojani (2023) note that this ensures differentiability. This approach is common and found in earlier work such as Akian, Menaldi and Sulem (1996), who likewise note that this ensures that the variable is continuous from origin in the positive real set.

aversion (CRRA) utility function³:

$$u(C_t) = \begin{cases} \frac{C_t^{1-\gamma}}{1-\gamma} & \text{if } \gamma \neq 1, \\ \log(C_t) & \text{if } \gamma = 1, \end{cases} \quad (5)$$

where C_t is consumption and c_t is the fraction of wealth W_t spent on consumption at time t . Hence $c_t = C_t/W_t$, and lowercase notation is henceforth used to denote variables as fractions of wealth. γ is the coefficient of relative risk aversion. The objective is to maximize the expected utility of consumption and wealth over the investor's lifetime:

$$\max_{\mathbf{x}_t, b_t, c_t} \mathbb{E} \left[\sum_{i=0}^{N-1} \beta^i u(C_i) \Delta t + \beta^N u(W_N) \right], \quad (6)$$

where β is the discount factor, \mathbf{x}_t is the allocation to risky assets, b_t is the allocation to the risk-free asset, and W_t is the investor's wealth at time t .

3.5 Intertemporal portfolio choice without transaction costs

When there are no transaction costs (no market frictions) the investor can freely rebalance the portfolio. This reduces the problem to the classic portfolio optimization problem formulated by (Merton 1969; Merton 1971). For a more detailed treatment, see (Björk 2019).

In this setting, the investor dynamically allocates wealth between D risky assets and a risk-free asset to maximize utility over a finite horizon $[0, T]$. The investor's wealth W_t can be allocated between a risk-free asset and D risky assets. Consumption is a non-durable good that can be purchased at each time point t . r is the risk-free rate, $\boldsymbol{\mu}$ is the vector of expected returns on the risky assets, and C_t represents consumption at time t . The investor's preferences follow a constant relative risk aversion (CRRA) utility function.

Without transaction costs, the optimal portfolio allocation, known as the Merton point is:

$$\mathbf{x}_t^* = \frac{1}{\gamma} \boldsymbol{\Sigma}^{-1} (\boldsymbol{\mu} - r), \quad (7)$$

where γ is the coefficient of relative risk aversion, and $\boldsymbol{\Sigma}$ is the covariance matrix of the risky assets' returns. This provides a time-independent optimal allocation that serves as a benchmark for models incorporating frictions such as transaction costs. This fraction is the optimal investment allocation, after consumption, to each risky asset and is independent of the wealth level. Merton also provides a closed form solution to the optimal consumption level. However this depends on wealth, and I find no relation to this and

³This is common in the literature. Other utility functions such as Epstein-zin preferences have been used but are less common.

my solutions later, so this is not covered.

3.6 The general class of dynamic portfolio choice with transaction costs and intertemporal consumption

Now consider when transaction costs are present, and the investor can consume a non-durable good at each time point. The solution to the dynamic portfolio choice problem is no longer given by the closed form solution of the Merton point. Considering the components presented in this section, the class of dynamic portfolio optimization problems, given one risk free asset and D risky assets, can be formulated by the following Bellman equation⁴:

$$V_t(W_t, \mathbf{x}_t, \theta_t) = \max_{c_t, \boldsymbol{\delta}_t^+, \boldsymbol{\delta}_t^-} \{u(c_t W_t) \Delta t + \beta \mathbb{E}_t [V_{t+\Delta t}(W_{t+\Delta t}, \mathbf{x}_{t+\Delta t}, \theta_{t+\Delta t})]\}, \quad t < T \quad (8)$$

Given some initial level of wealth W_0 and portfolio allocation \mathbf{x}_0 . θ_t is a vector of stochastic variables, which the gross one period risk free return, and risky return depends on, i.e $\mathbf{R}(\theta_t)$ and $R_f(\theta_t)$. These could cover the drift μ , volatility σ^2 , correlation of the risky assets Σ , and the risk free return r or only some of these, dependent on the model. Notice that future wealth and allocations are stochastic, as they depend on the future realization of θ_t .

Consumption and reallocation are decision variables, whereas bond holdings are not (explicitly). This is because bond holdings can be determined as the residual wealth, after consumption and reallocation decisions are made:

$$b_t W_t = \left(1 - \mathbf{1}^\top \cdot \mathbf{x}_t\right) W_t - \mathbf{1}^\top \cdot \boldsymbol{\delta}_t W_t - \psi(\boldsymbol{\delta}_t^+, \boldsymbol{\delta}_t^-, W_t) - c_t W_t \quad (9)$$

Where $\psi(\cdot)$ is the transaction cost function, and $\mathbf{1}$ is a vector of ones.

The dynamics of the state variables follow Schober, Valentin and Pflüger (2022) and are given by:

$$W_{t+\Delta t} = b_t W_t R_f(\theta_t) + ([\mathbf{x}_t + \boldsymbol{\delta}_t] W_t)^\top \cdot \mathbf{R}(\theta_t) \quad (10)$$

$$\mathbf{x}_{t+\Delta t} = \frac{((\mathbf{x}_t + \boldsymbol{\delta}_t) W_t) \odot \mathbf{R}_t(\theta_t)}{W_{t+\Delta t}} \quad (11)$$

Where \odot is the elementwise product (Hadamard product). The terminal value function is given by⁵:

$$V_T(W_T, \mathbf{x}_T, \theta_T) = u(W_T - \psi(\mathbf{x}_T W_T)) \quad (12)$$

⁴This is consolidated model of the base model, and with consumption model, of (Cai, Judd and Xu 2020), however the cost function is generalized and correlation of returns is included. For more on Bellman equations see (Bellman 1958)

⁵Stemming from the sum of discounted utility.

Which implies that the investor consumes everything at the terminal period, after moving investments to the deposit (bonds) account. Finally I note that the optimization problem is subject to the following constraints:

$$\delta_t W_t \geq -\mathbf{x}_t W_t \quad (13)$$

$$b_t W_t \geq 0 \quad (14)$$

$$\mathbf{1}^\top \mathbf{x}_t \leq 1 \quad (15)$$

The first constraint ensures that the investor does not short sell risky assets, The second is a no borrowing constraint constraint, or no shorting if b_t is viewed as a bond. The third is a no-leverage constraint (and no shorting / borrowing).

Furhtermore I note that the rebalancing decision (in each direction), is only feasible in the space, given the current allocation.:.

$$\delta_{i,t}^+ \in [0, 1 - x_{i,t}] \quad (16)$$

$$\delta_{i,t}^- \in [0, x_{i,t}] \quad (17)$$

This is a direct formulation of the constraints, already captured in the prior constraints. The problem can be simplified by normalizing with regard to wealth W_t , which removes W_t as a state variable, since wealth is seperable from the rest of the state space \mathbf{x}_t, θ_t as noted in (Cai, Judd and Xu 2013).

This is because portfolio optimality is independent of wealth for CRRA utility function under proportional costs⁶. The Bellman equation is then:

$$v_t(\mathbf{x}_t, \theta_t) = \max_{c_t, \delta_t^+, \delta_t^-} \{u(c_t)\Delta t + \beta \mathbb{E}_t \left[\pi_{t+\Delta t}^{1-\gamma} v_{t+\Delta t}(\mathbf{x}_{t+\Delta t}, \theta_{t+\Delta t}) \right] \}, \quad t < T \quad (18)$$

The normalized bond holdings are then:

$$b_t = 1 - \mathbf{1}^\top \cdot (\mathbf{x}_t - \delta_t - \psi(\delta_t^+, \delta_t^-)) - c_t \Delta t \quad (19)$$

This is still the residual of the wealth after the rebalancing and consumption decision. I still formulate the transaction cost function $\psi(\cdot)$ in terms of the buying and selling components, and use changes to allocations proportional to wealth, instead of the prior

⁶This will also be the case for my formulation of fixed costs.

formulations, where wealth was a direct input. The state dynamics are then:

$$\pi_{t+\Delta t} = b_t R_f(\theta_t) + (\mathbf{x}_t + \boldsymbol{\delta}_t)^\top \cdot \mathbf{R}(\theta_t) \quad (20)$$

$$\mathbf{x}_{t+\Delta t} = \frac{(\mathbf{x}_t + \boldsymbol{\delta}_t) \odot \mathbf{R}_t(\theta_t)}{\pi_{t+\Delta t}} \quad (21)$$

$$W_{t+\Delta t} = \pi_{t+\Delta t} W_t \quad (22)$$

I now formulate the problem with regard to the proportional wealth change $\pi_{t+\Delta t} = \frac{W_{t+\Delta t}}{W_t}$. The terminal value function is:

$$v_T(\mathbf{x}_T, \theta_T) = u(1 - \psi(\mathbf{x}_T)) \quad (23)$$

The constraints are likewise normalized:

$$\boldsymbol{\delta}_t \geq -\mathbf{x}_t \quad (24)$$

$$b_t \geq 0 \quad (25)$$

$$\mathbf{1}^\top \mathbf{x}_t \leq 1 \quad (26)$$

This class of dynamic portfolio choice problems covers most formulations of the problem, where the transaction cost specification is differentiable, and the utility function allows for separability of wealth and remaining state variables. If separability is not feasible, then the formulation with wealth as a state variable must be used, and the problem is more complex to solve. Since wealth denoted variables depend on prior wealth levels, and the problem is not separable over time.

Later formulations will be based on this class structure, covering the necessary Bellman equation, state dynamics, preferences and transaction costs functions as well as the constraints and any extensions not yet presented.

The non-normalized optimal choices can be obtained by multiplying the normalized choices with the wealth level W_t at a given time point t .

No closed form solution has been found for this class of problems with more than two risky assets. Numerical methods are required to solve the problem. The solutions to this problem are the optimal trading decisions and consumption, $\boldsymbol{\delta}_t^{+,*}, \boldsymbol{\delta}_t^{-,*}, c_t^*$. Optimal trading decisions for the problem, have been found to be the trading trajectory towards a region known as the NTR, which minimizes the euclidian distance between the allocation \mathbf{x}_t and the NTR (Cai, Judd and Xu 2013). The NTR is in this framework the set of asset allocations where it is sub-optimal to rebalance the portfolio, and is defined as:

$$\Omega_t = \{\mathbf{x}_t : \boldsymbol{\delta}_t^{+,*}, \boldsymbol{\delta}_t^{-,*} = \mathbf{0}\} \quad (27)$$

Where $\delta_t^{+,*}, \delta_t^{-,*}$ are the optimal buying and selling policies at time t . The NTR is central to this problem, as this region covers optimal trading decisions, and therefore every solution, when consumption is not included. When consumption is included, optimal consumption levels still need to be solved for and the problem is more complex. The next section will cover the NTR in more detail.

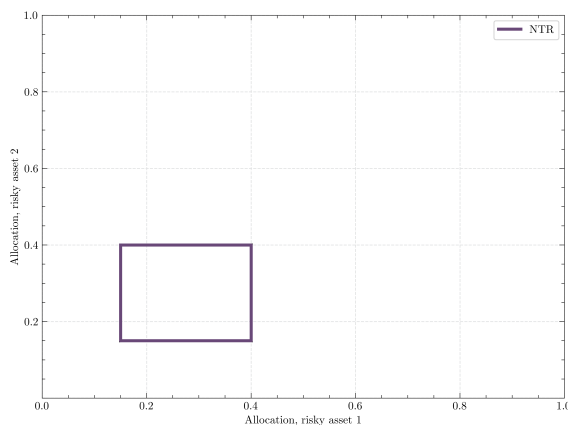
3.7 No Trade Region (NTR)

The NTR is a region in the risky asset space where it is sub-optimal to rebalance the portfolio. Given the parameters of the model the NTR without consumption is defined as in equation (27). If consumption is included, this definition remains the same, but the consumption decision may vary within the NTR. Note that the NTR is independent of the wealth level, but only depends on the wealth allocations. The NTR stems from the introduction of transaction costs, and is a connected set when the utility function is positively homogenous (Abrams and Karmarkar 1980). With proportional transaction costs, among others, the NTR has been found to be a convex set for static models (Dybvig and Pezzo 2020), and the same has been verified for dynamic models with proportional costs (Cai, Judd and Xu 2013).

The shape of the NTR is dependent on the parameters of the model, and can be a complex shape. With only proportional transaction costs and independent risky asset returns, the NTR for two risky assets is a square, as shown by Akian, Menaldi and Sulem (1996) among others. For one asset the NTR represent bounds on the relative allocation to the risky asset, as lines (Davis and Norman 1990).

The NTR may extend out of the feasible region, in which case the shape is truncated to the feasible space given the restrictions I set. For most cases seen in the literature, when consumption is not included, the NTR encapsulates the Merton point. Figure 3.1 illustrates an example of a NTR with two risky assets. The NTR is a key component of

Figure 3.1: Example No Trade Region with two risky assets.



the model, and illustrates the trade-off between the utility of rebalancing the portfolio and the cost of doing so. I will go into further detail on the NTR when covering the solution algorithm, where I will discuss the formal properties of the NTR, and how I can leverage key findings from the NTR to solve the dynamic portfolio choice problem with transaction costs efficiently.

3.8 Base problem: Portfolio choice with proportional costs and consumption

Considering the class of problems constructed in the prior section, I can now quickly introduce the basic problem formulation. I consider an investor with CRRA utility function. The investor can invest in one risk free asset and D risky assets. Trading is subject to proportional transaction costs hence I have the following cost function (in total trading volume):

$$\psi(\delta_{i,t}^+, \delta_{i,t}^-) = \tau(\delta_{i,t}^+ + \delta_{i,t}^-) \quad (28)$$

I do not assume that returns are dependent on stochastic parameters, but instead that they are drawn from a distribution with known parameters. Hence, I assume $\theta_t = \theta$ for all t . I assume a constant return on the risk free asset, i.e $R_f(\theta_t) = R_f$, and the risky assets follow a multivariate log-normal distribution, with some mean and covariance matrix. I can now formulate the entire problem given the class structure from section 3.6. The terminal value function is given by equation (23). The system is subject to the constraints of equations (24), (25) and (26), as well as a simple constrain on consumption, $c_t \geq 0$. I assume that the position in bond holdings is the residual wealth, and they therefore follow (19). The Bellman equation is therefore:

$$v_t(\mathbf{x}_t, \theta_t) = \max_{c_t, \delta_t^+, \delta_t^-} \{ u(c_t) \Delta t + \beta \mathbb{E}_t \left[\pi_{t+\Delta t}^{1-\gamma} v_{t+\Delta t}(\mathbf{x}_{t+\Delta t}) \right] \}, \quad t < T$$

With the same terminal condition as before, where investments are sold and wealth is consumed:

$$v_T(\mathbf{x}_T) = u(1 - \psi(\mathbf{0}, \mathbf{x}_T))$$

3.9 Portfolio choice with fixed costs

I now consider the model, where the investor faces fixed costs when rebalancing the portfolio, instead of proportional costs. Fixed costs are common in practice, and can be seen as a fixed fee for trading, regardless of the traded amount. I consider a slight modification to the purely fixed costs, and instead consider fixed costs as a percentage of the wealth. I do this to be able to use the same model structure as in section 3.8, where variables are in fractions of wealth, in order to drop wealth as a state variable.

This is seen previously in (Morton and Pliska 1995), who note that such a fixed cost

can be seen as a portfolio management fee. In practice, when setting the level of the fixed cost, I make an implicit assumption on the wealth of the investor, if I want to draw comparisons with pure fixed costs.

The cost function is then given by:

$$\psi(\boldsymbol{\delta}_t^+, \boldsymbol{\delta}_t^-) = \mathbf{1} \left(\sum_{i=1}^k \delta_{i,t}^+ + \delta_{i,t}^- > 0 \right) \cdot \text{fc} \quad (29)$$

Where fc is the fixed cost, and $\mathbf{1}(\cdot)$ is the indicator function. The fixed cost is only incurred if the investor rebalances the portfolio, and the cost is independent of the traded amount. The normalized bond holdings are therefore given by:

$$b_t = 1 - \mathbf{1}^\top \cdot (\mathbf{x}_t - \boldsymbol{\delta}_t) - \psi(\boldsymbol{\delta}_t^+, \boldsymbol{\delta}_t^-) - c_t \Delta t \quad (30)$$

The model otherwise remains the same as in section 3.8, with the same constraints and dynamics, while using the new cost function. Note, that in the terminal period, when all investments are sold, the fixed cost is incurred, unless the investor holds no risky assets. Note also, that the fixed cost function is not differentiable. Furthermore (Dybvig and Pezzo 2020) notes that the fixed cost problem is not a convex optimization problem, and is therefore not as easily solved as the proportional cost problem. I will deal with these issues individually when implementing the model.

3.10 Portfolio choice with fixed and proportional costs

The last model I consider is a combination of the two previous models, where the investor faces both fixed and proportional costs. This is a more realistic model, as it combines the two most common types of transaction costs an individual investor face on the financial markets. These could for example be a fixed brokerage fee and a percentage of the traded amount stemming from bid ask spreads, taxes or commisions (Lesmond, Ogden and Trzcinka 1999). The cost function is then given by:

$$\psi(\boldsymbol{\delta}_t^+, \boldsymbol{\delta}_t^-) = \mathbf{1} \left(\sum_{i=1}^k \delta_{i,t}^+ + \delta_{i,t}^- > 0 \right) \cdot \text{fc} + \tau(\boldsymbol{\delta}_t^+ + \boldsymbol{\delta}_t^-) \quad (31)$$

The normalized bond holdings are therefore given by:

$$b_t = 1 - \mathbf{1}^\top \cdot (\mathbf{x}_t - \boldsymbol{\delta}_t) - \psi(\boldsymbol{\delta}_t^+, \boldsymbol{\delta}_t^-) - c_t \Delta t \quad (32)$$

The model otherwise remains the same as in section 3.8, with the same constraints and dynamics, while using the new cost function.

4 Numerical implementation details

This section covers details regarding the solution algorithm and numerical implementation by (Gaegauf, Scheidegger and Trojani 2023). Each method is presented followed by the final solution algorithm which is presented lastly. This combines each of the methods. Methods span points sampling, numerical integration techniques, function approximation methods and solution techniques specific to this class of problems. Computational implementation is also presented, including the use of parallel computing and specific libraries in order to speed up the solution process.

4.1 Numerical integration

Consider the basic problem with proportional transaction costs, risky assets and a risk-free asset and no stochastic parameters. I need to evaluate the expectation of the value function: $\mathbb{E}[v_{t+\Delta t}(\mathbf{x}_{t+\Delta t})]$. In order to compute this expectation, I need to evaluate the integral:

$$\mathbb{E}_t \left[\pi_{t+1}^{1-\gamma} v_{t+1}(x_{t+1}) \right] = \int \pi_{t+1}^{1-\gamma} v_{t+1}(x_{t+1}) f(R_{t+1}), dR_{t+1} \quad (33)$$

where $f(R_{t+1})$ is the probability density function of the risky asset returns. If I look at the case of stochastic parameters, I would need to evaluate the conditional expectation with regard to these as well, given some distributional assumption on the parameters. The integral can be computed using Monte-carlo methods or by using quadrature rules.

4.1.1 Gauss-Hermite quadrature

Gaussian quadrature is a numerical integration method based on approximation and interpolation theory, and is a deterministic method. Gaussian quadrature can be used to approximate integrals using the following form, (Judd 1998):

$$\int_a^b f(x) w(x) dx \approx \sum_{i=1}^n \omega_i f(x_i), \quad (34)$$

Where ω_i are quadrature weights, x_i are quadrature nodes and $w(x)$ is a weighting function. This approximation is exact when $f(x)$ is a polynomial of degree $2n-1$ or less. Then I can approximate the integral using n points x_i and n weights ω_i . There are many different Gaussian quadrature schemes, with differing intervals $[a, b]$ and weighting functions $w(x)$. I consider the use of a Gauss-Hermite quadrature rule⁷, for a comprehensive review on quadrature rules, see (Judd 1998). Gauss-Hermite quadrature is used to approximate

⁷This is due to the distributional assumption of the returns, which is that these are log-normal

integrals of the form:

$$\int_{-\infty}^{\infty} f(x)e^{-x^2} dx \approx \sum_{i=1}^n \omega_i f(x_i) + \frac{n! \sqrt{\pi}}{2^n} \cdot \frac{f^{(2n)}(\zeta)}{(2n)!}, \quad (35)$$

Where $\zeta \in (-\infty, \infty)$. If a random variable X is normally distributed, i.e. $X \sim \mathcal{N}(\mu, \sigma^2)$, then I can compute the expectation, $\mathbb{E}[f(X)]$, which is given by:

$$\mathbb{E}[f(X)] = \frac{1}{\sqrt{2\pi\sigma^2}} \int_{-\infty}^{\infty} f(x)e^{-\frac{(x-\mu)^2}{2\sigma^2}} dx \quad (36)$$

Using a change of variables $y = \frac{x-\mu}{\sqrt{2}\sigma}$. I then rewrite the expectation on the form of the Gauss-Hermite quadrature rule:

$$\mathbb{E}[f(X)] = \frac{1}{\sqrt{2\pi\sigma^2}} \int_{-\infty}^{\infty} f(\sqrt{2}\sigma y + \mu) e^{-y^2} \sqrt{2}\sigma dy \quad (37)$$

$$= \frac{1}{\sqrt{\pi}} \int_{-\infty}^{\infty} e^{-y^2} f(\sqrt{2}\sigma y + \mu) dy \quad (38)$$

$$\approx \frac{1}{\sqrt{\pi}} \sum_{i=1}^n \omega_i f(\sqrt{2}\sigma x_i + \mu) \quad (39)$$

Where ω_i are the quadrature weights, x_i are the quadrature nodes over the interval $(-\infty, \infty)$.

When X is log-normal, i.e $\log X \sim \mathcal{N}(\mu, \sigma^2)$, then I can use a variable change once again: $X = e^Y$ and $Y \sim \mathcal{N}(\mu, \sigma^2)$. I can then rewrite the expectation as:

$$\mathbb{E}[f(X)] = \mathbb{E}[f(e^Y)] \approx \pi^{-\frac{1}{2}} \sum n_{i=1} \omega_i f\left(e^{\sqrt{2}\sigma x_i + \mu}\right) \quad (40)$$

To extend this framework to multiple dimensions I can use product rules as noted by (Judd 1998). Consider Y which is multivariate normal, i.e $Y \sim \mathcal{N}(\boldsymbol{\mu}, \Sigma)$, where $\boldsymbol{\mu}$ is the drift vector and Σ is the covariance matrix. Let L be a lower-triangular matrix such that $LL^\top = \Sigma$ (Cholesky factorisation). Then I have that:

$$\mathbb{E}\{f(Y)\} = \left((2\pi)^d \det(\Sigma)\right)^{-\frac{1}{2}} \int_{\mathbb{R}^d} f(y) e^{-\frac{1}{2}(y-\boldsymbol{\mu})^\top \Sigma^{-1}(y-\boldsymbol{\mu})} dy \quad (41)$$

$$= \left((2\pi)^d \det(L)^2\right)^{-\frac{1}{2}} \int_{\mathbb{R}^d} f\left(\sqrt{2}Ly + \boldsymbol{\mu}\right) e^{-\frac{1}{2}y^\top y} dy \quad (42)$$

$$\begin{aligned} &\approx \pi^{-\frac{d}{2}} \sum_{i_1=1}^n \cdots \sum_{i_d=1}^n \omega_{i_1} \cdots \omega_{i_d} f\left(\sqrt{2}L_{1,1}y_{i_1} + \mu_1, \right. \\ &\quad \left. \sqrt{2}(L_{2,1}y_{i_1} + L_{2,2}y_{i_2}) + \mu_2, \dots, \sqrt{2}\left(\sum_{j=1}^d L_{d,j}y_{i_j}\right) + \mu_d\right) \end{aligned} \quad (43)$$

Where d refers to the number of dimensions, n is the number of quadrature points, ω_i are the quadrature weights and y_i are the quadrature nodes. $L_{i,j}$ is the i th row and j th column of the Cholesky factorisation matrix L . $\det(\cdot)$ is the matrix determinant. Note that the use of product rules suffers from the curse of dimensionality, as the complexity scales exponentially with the number of dimensions. This is because the quadrature points with the product rule, use a tensor product grid, which is constructed using the Cartesian product of the quadrature points in each dimension. I can use sparse grid methods to partially tackle this. One common method is the Smolyak method, (Smolyak 1963). The Smolyak sparse grid method approximates multidimensional integrals, over dimension d while limiting the amount of points used. The method is composed of the following:

1. **Univariate Quadrature Rules:** Each dimension of the integration domain is assigned a univariate quadrature rule, which provides both nodes (quadrature points) and weights for numerical integration in that dimension. The accuracy of each rule is determined by its *level*, denoted by i_d for each dimension d . The level determines the number of quadrature points in that dimension, which improves the accuracy of the quadrature rule.
2. **Approximation Level (μ):** The accuracy of the Smolyak sparse grid is controlled by the *approximation level* μ . This parameter sets a limit on the sum of levels across all dimensions, controlling the total number of grid points. Higher values of μ result in more accurate approximations but increase computational complexity.
3. **Multi-Index and Combination of Levels:** In a d -dimensional integral, the Smolyak method uses a *multi-index* $i = (i_1, i_2, \dots, i_d)$ to represent the level of the quadrature rule in each dimension. The multi-index specifies a unique combination of quadrature levels for each dimension, where i_d denotes the level for dimension d . To construct a sparse grid, Smolyak's method restricts the sum of these levels using the following condition:

$$d \leq i_1 + i_2 + \dots + i_d \leq d + \mu$$

This constraint on the sum of levels, reduces the number of tensor products. I denote the sum of multi indicies: $|i| = i_1 + i_2 + \dots + i_d$.

4. **Tensor Product of Univariate Rules:** The Smolyak grid is formed by taking the *tensor product* of univariate quadrature rules that satisfy the multi-index constraint. Each univariate quadrature rule, represented by Q_{i_d} at level i_d in dimension d , is combined across dimensions according to the set of multi-indices i .

This combination is given by:

$$A(\mu, d) = \sum_{d \leq |i| \leq d+\mu} (-1)^{\mu+d-|i|} \binom{d-1}{\mu+d-1-|i|} \bigotimes_{d=1}^{|i|} Q_{i_d}$$

where:

- Q_{i_d} is the univariate quadrature rule at level i_d in dimension d ,
- \bigotimes denotes the tensor product, and
- $\binom{d-1}{\mu+d-1-|i|}$ is a combinatorial coefficient that assigns weights to each tensor product, for accurate integration up to the specified approximation level μ .

By restricting the multi indices i with the approximation level μ , the Smolyak method reduces the number of points needed for numerical integration in higher dimensions. Tensor grid methods grow exponentially with the number of dimensions d , the Smolyak grid grows polynomially, (Judd et al. 2014). Hence this directly tackles the curse of dimensionality. For more on this see (Smolyak 1963), (Judd et al. 2014) and (Horneff, Maurer and Schober 2016).

4.1.2 Monte Carlo integration (MC)

Monte Carlo integration is a numerical integration method based on *sampling*, as opposed to quadrature rules which are based on interpolation.

The convergence of Monte Carlo integration is generally slower than some quadrature methods; however, its convergence rate is independent of the dimensionality of the integral, making it well-suited for high-dimensional problems. Monte Carlo integration breaks the curse of dimensionality. Monte Carlo (MC) integration is based on random sampling⁸ over the domain of the integral, and then computing the sample average of the function to be integrated. Lets say I want to approximate the d -dimensional integral:

$$I = \int_{\Omega} f(\mathbf{x})g(\mathbf{x})d\mathbf{x} = \mathbb{E}[f(\mathbf{x})], \quad (44)$$

where $g(\mathbf{x})$ is the probability density function of the random variable \mathbf{x} over its support Ω . I approximate I as:

$$Q_N = \frac{1}{N} \sum_{i=1}^N f(\mathbf{X}_i), \quad (45)$$

where \mathbf{X}_i are independent samples drawn from $g(\mathbf{x})$. The procedure is then:

1. Sample N points $\mathbf{x}_1, \dots, \mathbf{x}_N$ from $g(\mathbf{x})$.

⁸Strictly speaking the samples are not random, but pseudo-random, meaning that deterministic samples are used, which appear random. For more in this see (Judd 1998) or (Glasserman 2004).

2. Approximate the expectation $\mathbb{E}[f(\mathbf{x})]$ by the sample average:

$$I \approx Q_N = \frac{1}{N} \sum_{i=1}^N f(\mathbf{x}_i).$$

The Law of Large Numbers ensures that the sample average converges to the mean as $N \rightarrow \infty$:

$$\lim_{N \rightarrow \infty} Q_N = \mathbb{E}[f(\mathbf{x})] = I.$$

And by the Central Limit Theorem, I have:

$$\sqrt{N}(Q_N - I) \xrightarrow{d} N(0, \sigma^2),$$

where $\sigma^2 = \text{Var}[f(\mathbf{x})]$ does not depend on N or d . The standard error of Q_N is:

$$\sigma_{Q_N} = \frac{\sigma}{\sqrt{N}}.$$

The convergence rate of $1/\sqrt{N}$ is independent of the dimension.

4.1.3 Quasi-Monte Carlo integration (QMC)

Quasi-Monte Carlo integration substitutes the 'random' samples in Monte Carlo integration with specific deterministic sequences such as equidistributed sequences, Low-Discrepancy Sequences (LDS) or Lattice point rules etc. I will focus on the use of low discrepancy sequences. For a comprehensive review of sequences and rules see (Judd 1998).

LDS are deterministic sequences which cover the domain of the integral more evenly than random samples. Discrepancy is in this case a measure of deviation from perfect uniformity over the domain of the integral. Thus to go from MC in (45) to QMC, I replace the random samples \mathbf{X}_i with LDS samples. I note that the sampling of the QMC is now dependent on the dimensionality of the integral, as opposed to MC, as the LDS samples have to be drawn with respect to the dimensionality of the integral.

I consider two different types of LDS sequences, the Halton sequence and the Sobol sequence. Both sequences are popular LDS sequences, which are used in Quasi-Monte Carlo (QMC) applications (Glasserman 2004).

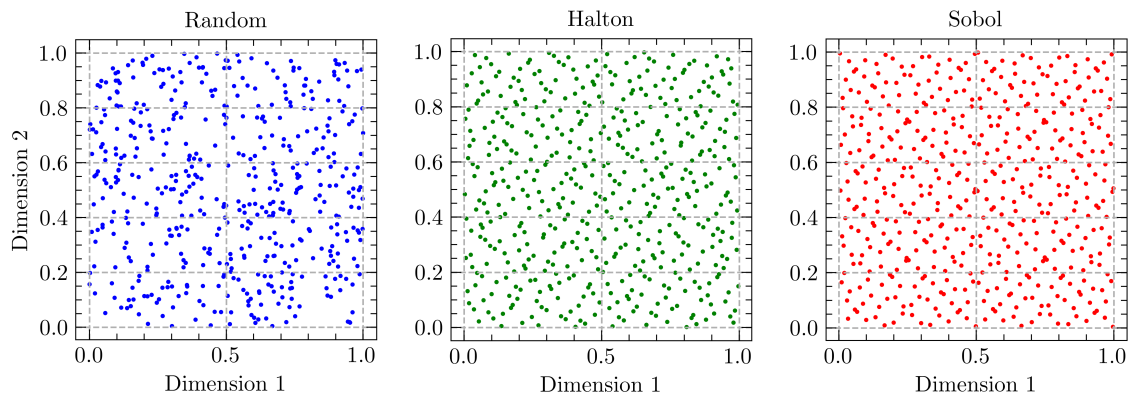
The convergence rate of QMC is:

$$\frac{(\log N)^d}{N} \tag{46}$$

Hence QMC is generally faster than MC, e.g $\frac{(\log N)^d}{N} < \frac{1}{\sqrt{N}}$ for large N and small d . I note that as dimensionality d increases, the quality of the Halton sequence decreases, as the dimensions become more correlated, (Glasserman 2004). Specifically the Halton

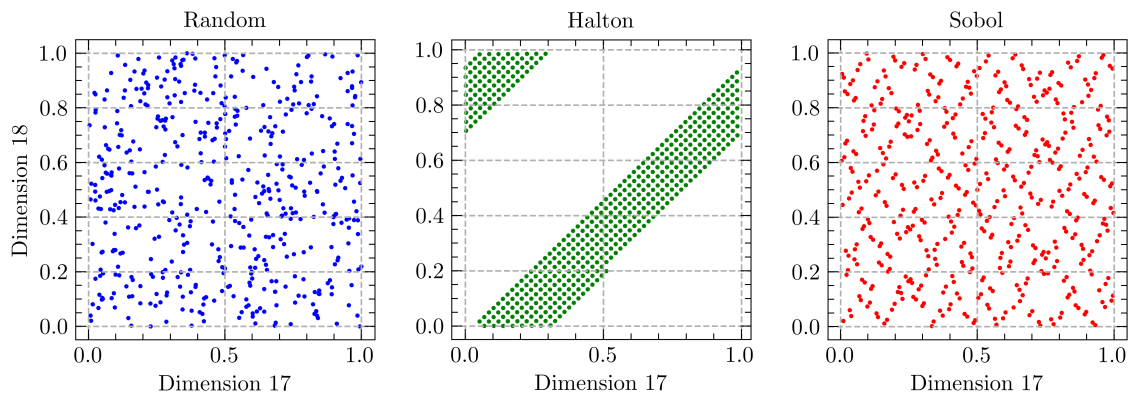
sequence will produce diagonal points when projected onto a 2D plane. This is displayed in Figure 4.1. I therefore prefer the Sobol sequence when the dimensionality is sufficiently high, and as not to complicate matters, also use the Sobol sequence in lower dimensions, when QMC schemes are used. The figures below show random samples, Halton samples and Sobol samples in 2d. the second figure shows the same in 18 dimensions. Halton shows that dimension 17 and 18 are correlated.

Figure 4.1: Comparison of sample generation for Monte Carlo and Quasi-Monte Carlo



Note: Each sequence was generated using $N = 500$ samples and $d = 2$ dimensions.

Figure 4.2: Comparison of sample generation for Monte Carlo and Quasi-Monte Carlo with increased dimensionality



Note: Each sequence was generated using $N = 500$ samples and $d = 18$ dimensions.

QMC is generally found to be more efficient than MC, as noted by (Glasserman 2004), (Judd 1998), and notably Glasserman find that dimensionality has to be quite large before the Monte Carlo method is favorable to the quasi Monte Carlo method. Furthermore,

Glasserman find that while generally N must by increase a lot when d is increased, this is not always the case in financial applications, as the integrals employed in these examples can often be approximated by integrals of much lower dimension. QMC therefore performs better than to be expected.

However I note that QMC lacks a straightforward variance estimator, a feature recovered through *randomized QMC*, which will be discussed in the next section.

4.1.4 Randomized Quasi-Monte carlo integration (RQMC)

Randomized quasi-Monte Carlo integration (RQMC) is a combination of QMC and MC integration. I consider the the QMC integral, i.e the equation of (45), using an LDS sequence. The point of Randomized Quasi-Monte Carlo (RQMC) is then to introduce randomness to the sequence: $P_n = \{x_1, \dots, x_n\}$. I will cover the most simple case, *Random shift* and *Scrambling* methods, however for a comprehensive review of randomization methods see Glasserman (2004). The most simple method of randomizing P_n is to add a *random shift* to each point in the sequence, using random numbers drawn from a uniform distribution of the same dimensionality as the sequence, wrapped to the interval of P_n .

Hence, if $x_i \in [0, 1)^d$ then I add a random shift $u_i \bmod 1$, where $\bmod 1$ keeps the shift within the interval $[0, 1)$. A major disadvantage of the random shift is that it changes the discrepancy properties of the sequence, and thus the quality of the sequence is lost.

Scrambled nets is a method of randomization which can be applied to LDS sequences specifically. Scrambling works by applying a sequence of random permutations to the digits in the base- b representation of each coordinate in the LDS. Each digit is permuted based on the values of the digits that came before it. This structure retains the low-discrepancy properties while introducing a controlled level of randomness, which enables the calculation of variance for RQMC estimates. In multi-dimensional settings, this scrambling is applied independently to each coordinate of the sequence, allowing us to estimate variance across the entire space. Scrambling the Sobol sequence has been found to be particularly effective in financial applications, as noted by (Hok and Kucherenko 2023). QMC is generally more efficient than MC, and RQMC increases the rate of convergence of QMC and allows for the estimation of variance.

4.1.5 Choice of numerical integration technique

Given the number of points needed for Monte-carlo methods I will usually use the Gauss-Hermite quadrature rule for the case of log-normal returns. This holds the distinct advantage of being deterministic, and hence the same result is obtained each time the integral is computed. The Monte-Carlo method can likewise be deterministic when implemented, for more on this see the literature on random number generators. Monte-Carlo methods will be considered, when the number of dimensions is sufficiently large, and the

number of points needed for the Gauss-Hermite quadrature rule is too large, however, such cases are not feasible with the computational resources available to me. However the Monte-carlo methods are recommended, should higher dimensions be considered.

4.2 Value function approximation

This section covers the necessary function approximation method used in the solution algorithm, which uses machine learning techniques. I cover the use of GPR, in order to approximate the value function of the dynamic portfolio allocation problem, following (Gaegau, Scheidegger and Trojani 2023). Competing methods will be discussed later.

4.2.1 Gaussian process regressions (GPR)

A Gaussian process (GP) is a Probabilistic Machine Learning (PML) model that defines a distribution over functions used to make predictions based on data. The GP is specified by two functions: the mean function and the covariance function, also called the kernel. The mean function, $\mu(\mathbf{x})$, represents the expected value of the function at a given input \mathbf{x} , and the covariance function, $k(\mathbf{x}, \mathbf{x}')$, captures the covariance between function values at different input points \mathbf{x} and \mathbf{x}' . In a GP, any finite set of input points $\mathbf{X} = (\mathbf{x}_1, \dots, \mathbf{x}_N)$ within the domain \mathbb{R}^d results in the function values $\mathbf{f} = (f(\mathbf{x}_1), \dots, f(\mathbf{x}_N))$ having a joint multivariate Gaussian distribution. This property enables a GP to provide a prior distribution over functions based on the defined mean and covariance.

I use GPR to estimate the value function in the dynamic portfolio allocation problem, when I am not at the terminal decision period⁹, i.e., $t < T - 1$, following (Gaegau, Scheidegger and Trojani 2023). The GP is formulated by the previously mentioned mean and covariance functions:

$$f(\mathbf{x}) \sim \mathcal{GP}(\mu(\mathbf{x}), k(\mathbf{x}, \mathbf{x}')), \quad (47)$$

The covariance kernel function $k(\mathbf{x}, \mathbf{x}')$ can be any Mercer kernel, i.e., positive definite (Murphy 2023). Common kernel choices include the Radial Basis Function (RBF) kernel, the Matern kernel, and the Exponential kernel. I employ a Matern kernel, which, depending on the parameter ν , can be a generalization of the RBF kernel or the Exponential kernel. This choice follows (Gaegau, Scheidegger and Trojani 2023). The Matern kernel is given by:

$$k_{\text{Matern}}(\mathbf{x}, \mathbf{x}') = \frac{2^{1-\nu}}{\Gamma(\nu)} \left(\frac{\sqrt{2\nu} \|\mathbf{x} - \mathbf{x}'\|_2}{\ell} \right) K_\nu \left(\frac{\sqrt{2\nu} \|\mathbf{x} - \mathbf{x}'\|_2}{\ell} \right), \quad (48)$$

where $\|\cdot\|_2$ is the Euclidean norm, Γ is the gamma function, and K_ν is the modified Bessel function. The length scale ℓ and smoothness parameter ν are both positive. As $\nu \rightarrow \infty$,

⁹At $t = T - 1$, I know that v_{t+1} is the terminal value function.

the Matern kernel converges to the RBF kernel (Gonzalvez et al. 2019). Functions from this class are k -times differentiable when $\nu > k$. When $\nu = 1/2$, the Matern kernel corresponds to the Ornstein-Uhlenbeck process (Murphy 2023), which is commonly used in financial applications, such as models of interest rates (Glasserman 2004). The choice of kernel is done to replicate the framework of (Gaegau, Scheidegger and Trojani 2023), and is found to perform well.

I now introduce the GP model in the context of the dynamic portfolio allocation problem. Consider a training dataset $\{\mathbf{X}, \mathbf{y}\}$ with N points \mathbf{x}_i and observed values \mathbf{y} . These are the allocations and trading decisions and consumption, and the corresponding value function. I assume that the observations \mathbf{y} are generated by an unknown function f , such that

$$y_i = f(\mathbf{x}_i) + \varepsilon_i, \quad \varepsilon_i \sim \mathcal{N}(0, \sigma_\varepsilon^2),$$

where σ_ε^2 represents the observational noise¹⁰. Observational noise is due to numerical instability, measurement errors, or other factors that introduce uncertainty into the observations, such as the tolerance level of the optimization algorithm. The goal is to train a GP on this dataset and then use it to predict the value function at a new state \mathbf{x}_* , yielding a new predicted output f_* .

The training observations \mathbf{y} and the predicted noise-free function f_* have a joint Gaussian distribution:

$$\begin{bmatrix} \mathbf{y} \\ \mathbf{f}_* \end{bmatrix} \sim \mathcal{N} \left(\mathbf{0}, \begin{bmatrix} k(\mathbf{X}, \mathbf{X}) + \sigma_\varepsilon^2 \mathbf{I} & k(\mathbf{X}, \mathbf{x}_*) \\ k(\mathbf{x}_*, \mathbf{X}) & k(\mathbf{x}_*, \mathbf{x}_*) \end{bmatrix} \right) \quad (49)$$

Here I have assumed a zero mean function¹¹, and the kernel function is the Matern kernel. The posterior distribution of the predicted value function f_* given the training data is then a multivariate normal, (Murphy 2023), with mean:

$$\tilde{\mu}(\mathbf{x}) = k(\mathbf{x}_*, \mathbf{X})[k(\mathbf{X}, \mathbf{X}) + \sigma_\varepsilon^2 \mathbf{I}]^{-1} \mathbf{y}, \quad (50)$$

And covariance:

$$\tilde{k}(\mathbf{x}_*, \mathbf{x}'_*) = k(\mathbf{x}_*, \mathbf{x}'_*) - k(\mathbf{x}_*, \mathbf{X})[k(\mathbf{X}, \mathbf{X}) + \sigma_\varepsilon^2 \mathbf{I}]^{-1} k(\mathbf{X}, \mathbf{x}'_*) \quad (51)$$

Therefore in order to predict the value function at a new state \mathbf{x}_* , I need to compute the mean and covariance. This step is computationally burdensome as I have to compute the four large covariance matrices in the joint distribution (49). Afterwards I can compute

¹⁰The noise assumption implies that the GP model does not interpolate the data but rather fits a smooth function. This results in computational costs of $O(N)$ for the mean prediction and $O(N^2)$ for the variance prediction. For more details, see (Murphy 2023). Complexity is actually larger for the implementation available to me.

¹¹This does not imply that the actual data has mean zero, but it provides nice properties of the GP (Murphy 2023).

predictions using the mean function (50) and the covariance function (51) can be used to compute error bands on the predictions.

As noted, training and predicting with a GP is computationally expensive. I will therefore introduce the methods employed to reduce the computational burden of the GP. I use automatic relevance detection (ARD) which is a modification to the Matern kernel to use a length scale for each dimension, ℓ_i . Dimensions with low impact has a high length scale, and are effectively ignored. Note that this is not the same as Lasso, as these coefficients are not set to 0.

For high dimensional problems the use of Structured Kernel Interpolation for Products (SKIP), could be employed see (Pleiss et al. 2018) which would reduce the computational burden of computing the matrices in the joint distribution (49), however this is not implemented.

4.3 Approximating the No trade region

Since I now have introduced methods to approximate the next-period value function v_{t+1} , and methods for evaluating the expectation $\mathbb{E}[\cdot]$ over known distributions, I can now approximate the NTR using a DP scheme. In order to do this some assumptions regarding the unknown NTR are formed. These are drawn directly from (Gaegau, Scheidegger and Trojani 2023)

Assumption 1. *The NTR is a D -dimensional convex polytope.*

A polytope is a generalization of a polyhedron (polytope in two dimensions), which is a geometric object with flat sides and straight edges. The convex polytope is a polytope which bounds a convex set, and can therefore be defined by a convex hull. Thus, any linear combination of points in the NTR or on the boundary of the NTR is also in the NTR. In other words, the NTR is a closed convex set.

Assumption 2. *The NTR has 2^D vertices.*

This assumption is regarding the shape of the NTR. Note, that if the actual NTR has less than 2^D vertices, the approximation will be close to the actual shape, as the approximated vertices will be on top of each other. However if the NTR has more than 2^D vertices, then the approximation will be a simplification of the actual shape.

The existing literature has found that the NTR is a D -dimensional square / parallelogram, this is formally shown with uncorrelated assets by (Liu 2004). With correlated assets the same is found by (Cai, Judd and Xu 2013; Dybvig and Pezzo 2020). Hence, I believe this sampling scheme to be sufficient for the case of proportional transaction costs. (Dybvig and Pezzo 2020) find that the NTR is a circle or ellipse when there are only fixed costs, and when there are asset specific costs the NTR is a hexagon with two assets, as one vertice is added per asset.

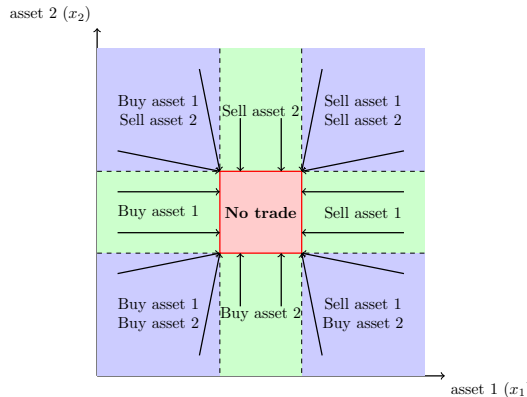
This would suggest other sampling schemes for these cases, leveraging the new geometric shapes. For the circular case I would need to find the center-point and the radius of the circle in order to define the NTR, irrespective of dimensions $D > 1$.

If this is not possible I would need to sample evenly around the circle (sphere / hypersphere), this problem is well known in mathematics and computer graphics and many methods for this exists, among others lattice point methods. For more on this see for example (Bono, Nicoletti and Ricci-Tersenghi 2024). However the complexity for such a solution increases in dimensionality, and especially when correlation is added, since this would shift the circle to an ellipse (Dybvig and Pezzo 2020).

For the hexagonal case, I could add more midpoints between the vertices of the existing sampling scheme, however this assumes straight lines connecting the vertices still. I tackle these cases later and proceed with the general case of the NTR as a convex polytope, under proportional costs. With these two assumptions in place, a strategy for approximating the NTR can be formed with few initial points. Given assumption 2, I can approximate the NTR by using 2^D points, which are the vertices of the NTR, and by assumption 1, I can approximate the NTR by using the outer convex hull of these points, i.e connecting the vertices by straight lines. I can leverage the following intuition from (Gaegauf, Scheidegger and Trojani 2023), and from Figure 3.1.

For any point outside the NTR, the optimal policy is to trade towards the boundary of the NTR. Since each point on the boundary of the NTR is optimal, the optimal trading route minimizes the distance, and hence the optimal trading route is a straight line to the boundary of the NTR. If the points are chosen correctly, the optimal trading route will be directly to the nearest vertex of the NTR.

Figure 4.3: Schematic of the No-Trade Region



This figure is a recreation of Figure 1. in Gaegauf, Scheidegger and Trojani (2023).

In Figure 4.3, blue regions are regions where optimal policy δ is to adjust in both assets. Green regions are regions where the optimal policy is to hold in one asset and adjust the

other. If one considers the example in Figure 4.3, I can effectively approximate the NTR, by sampling a point in each of the blue regions, and then solving the optimization problem to find the vertices. When the NTR is unknown, sampling from the blue regions seem difficult at a first glance. However, I can sample the vertices of each simplex that covers the feasible space, and the midpoints between these. By this I mean the corners of the feasible space, as well as the portfolio of evenly distributed allocation of the assets. This sampling scheme leads to the following points in the 2-dimensional case:

$$\begin{bmatrix} 0 & 0 \\ 1 & 0 \\ 0 & 1 \\ 0.5 & 0.5 \end{bmatrix}$$

Extensions of this sampling scheme to higher dimensions is trivial. This should effectively cover the feasible space and allow for approximating the NTR. Note, that this sampling scheme only covers NTR with no borrowing, and no short-selling as noted in (Gaegau, Scheidegger and Trojani 2023). If borrowing and short-selling were introduced, I would have to set some bounds on the borrowing and short-selling, and then sample from these bounds. Effectively creating a triangle / prism, around the feasible space, and then sample the outer borders of this space.

Having approximated the NTR, I can now use this in the solution algorithm. There are two main ways which the NTR approximation can be leveraged in order to lessen the computational burden of the solution algorithm. These will be covered next.

4.3.1 Strategic point sampling

After having approximated the NTR, I need to efficiently approximate the value function in the time step related to the NTR. This is done by sampling points over the entire feasible space and then solving for the optimal trade route for each point.

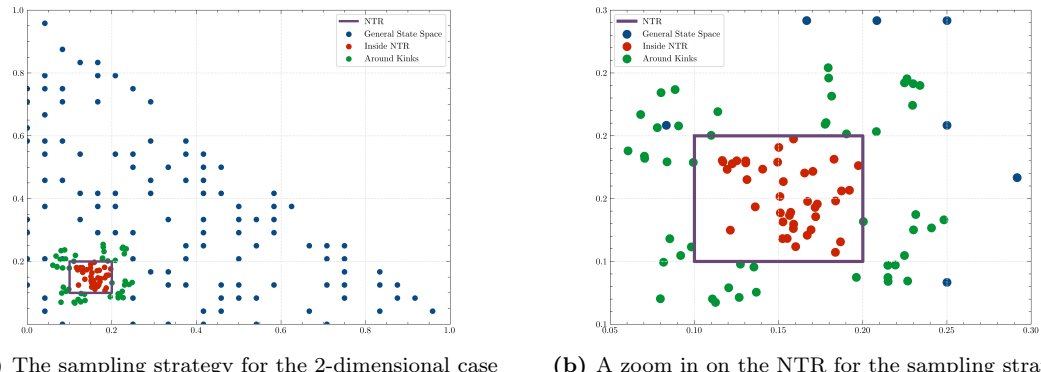
In order to ensure that the approximation of the value function is of high quality, and that this value function can effectively be used for any point in the state space, I need to ensure that the points are sampled in a strategic manner. This means I need points of a few different types. I need points inside the NTR, and around the NTR in any direction, and various distances to the NTR. This leads to three types of points I need to sample: *Points inside the NTR, points near the kinks of the NTR and points in the general state space, outside the NTR*. An easily implementable solution is to use a naive grid sampling method, such as uniform draws over the feasible state space, or to use a grid-method which evenly covers the feasible state space. However, a simple naive grid method for sampling points over the state-space has a few drawbacks which I need to tackle.

Firstly, a naive grid method, such as uniform draws, will not cover the NTR efficiently,

especially for small NTRs. I would need a large amount of grid points to be sure that there are multiple points inside the NTR. A pure random grid would likewise need a large amount of points, in order to cover the NTR efficiently, especially in each direction around the NTR. Both of these methods, and a schematic NTR are shown in appendix A. I therefore instead, follow the method of (Gaegauf, Scheidegger and Trojani 2023), and sample points in a strategic manner. This scheme consists of the three point types mentioned earlier, with a sampling method for each of these points. Having approximated the NTR, I can effectively sample point in this manner:

1. Sample points outside the NTR in the general state space using a uniform grid. I then remove all points inside the NTR, and sample random points from the grid until I have enough points.
2. Sample points inside the NTR. For this I consider random draws, as the placement inside the NTR is not of high importance. I just need enough to approximate the value function.
3. Sample points around the NTR kinks. For this I consider each NTR vertice. I then interpolate between vertices slightly, and extend these outward with random positive noise draws.

Figure 4.4: The designed sampling strategy for state space coverage.



Note: Sample consists of $N = 200$ points, with 122 blue points in the general state space (55%), 40 red points inside the NTR (20%) and 48 green points around the NTR kinks (25%).

The resulting points are plotted in Figure 4.4a, and a zoom in on the NTR and its kinks are shown in Figure 4.4b. (Gaegauf, Scheidegger and Trojani 2023) find that especially increased sampling around the kinks, leads to a better approximation of the value function, and $N > 100$ points leads to sufficient approximations for dimensions $D \leq 5$, as most of the approximation error is due to the kinks of the NTR.

This choice of sampling scheme reduces the strain of the curse of dimensionality, as grid sampling schemes would increase the number of points exponentially with the number of dimensions. Note, that while this scheme still increases the number of points needed with the dimensionality, the oversampling of kink points especially reduce the number of points needed in higher dimensions.

4.3.2 Utilizing the NTR approximation for δ bounds

Having constructed an efficient sampling strategy, I can further leverage the NTR approximation to find bounds on the optimal policy $\boldsymbol{\delta}$, for the optimization step for each of these points. For this, consider the schematic NTR in Figure 4.3. At each point outside the NTR, the optimal policy is to trade towards the boundary of the NTR. This can either mean trading towards a vertice of the NTR or one of the faces. For the blue regions, trading towards a vertice is optimal, and this means that the optimal policy is to reallocate in both risky assets.

In this case, I can set bounds on the optimal policy $\boldsymbol{\delta}$, by considering the direction which minimizes the euclidian distance to the NTR. If I know beforehand, that for asset 1 the investor needs to sell (lower-right blue region), then I can set bounds on δ_1^+ to 0 and effectively remove this from the optimization problem. I can likewise do this the other way around for asset 2, which the investor needs to buy more of, and set bounds on δ_2^- to 0.

For the green regions in the figure, the optimal policy is to trade towards a face of the NTR, and this means that the optimal policy is to reallocate in one risky asset and hold the other. I can therefore set bounds on the optimal policy δ_i to 0 for the asset which is to be held, and only consider reallocation in the second asset¹².

This method of setting bounds on the optimal policy $\boldsymbol{\delta}$ is a way to reduce the computational burden of the optimization problem, and to ensure that the optimization problem is well defined. Furthermore, by knowing that the optimal policy reduces the euclidian distance to the NTR, I can effectively remove policies which would suggest buying and selling the i th asset (only trade in straight lines).

4.3.3 Multiple Gaussian Process Regressions

The final ingredient in the algorithm is the use of multiple GPRs. Since I now can effectively sample points, and have information on their placement relative to the NTR, I can leverage this and estimate two separate value functions, one inside the NTR and one outside the NTR. This strategy effectively deals with the kinks of the NTR, as this otherwise would pose a problem for any smooth function approximations. I construct one GP for the points inside the NTR, and one for the points outside the NTR, and when

¹²Bounds on both δ^+ and on δ^- .

I then evaluate the value function at a point $v_{t+1}(\mathbf{x}_{t+1})$, I select the appropriate GP to evaluate the value function.

This is done after having optimized over the N points from the sampling strategy. I then construct two datasets:

$$\mathbf{X}_{t,\text{inside}} = \{\mathbf{x}_{t,i}, \hat{v}_{t,i} \mid \mathbf{x}_{t,i} \in \hat{\Omega}_t\} \quad (52)$$

$$\mathbf{X}_{t,\text{outside}} = \{\mathbf{x}_{t,i}, \hat{v}_{t,i} \mid \mathbf{x}_{t,i} \notin \hat{\Omega}_t\} \quad (53)$$

Then each GP is fit over the dataset, which consists of asset allocations and the corresponding value function output. In the next period, $t - 1$ (since I iterate backwards), I can then evaluate the next period value function $v_{t+1}(\mathbf{x}_{t+1})$, by selecting the appropriate GP, and using the predictive mean from (50):

$$\tilde{\mu}(\mathbf{x}_{t+1}) = k(\mathbf{x}_{t+1}, \mathbf{X}_{t+1})[k(\mathbf{X}_{t+1}, \mathbf{X}_{t+1}) + \sigma_\epsilon^2 \mathbf{I}]^{-1} \hat{\mathbf{v}}_{t+1}, \quad (54)$$

4.4 Final solution algorithms

Now that each component regarding the solution algorithm has been covered, I now present the solution algorithms for the dynamic portfolio allocation problem in pseudo code. Starting at the second to last period, which is the last period where the investment decision is not trivial, the algorithm is as follows: Sample 2^D points to approximate the NTR. Then Approximate the NTR by solving the optimization problem for these points.

Sample N points in a strategic manner as described in Section 4.3.1. For each $x_{i,t} \in X_t$ with $\{X_t\}_{i=1}^N$, solve the optimization problem to find the optimal policy δ_i .

Construct the datasets $\mathbf{X}_{t,\text{inside}}$ and $\mathbf{X}_{t,\text{outside}}$ and fit two GPRs to the datasets $\mathbf{X}_{t,\text{inside}}$ and $\mathbf{X}_{t,\text{outside}}$. The code can be split into two parts, algorithm (A) and algorithm (B). Algorithm A covers approximation the NTR and algorithm B covers the entire DP scheme. These are drawn from the framework which has been covered above, originally created by (Gaegau, Scheidegger and Trojani 2023).

Algorithm 1. Approximate the t -th period NTR in the discrete-time finite-horizon portfolio choice model with proportional transaction costs.

```

Input :  $t + 1$  period's value function approximation  $V_{t+1}$ .
Result : Set of approximated NTR vertices:  $\{\hat{\omega}_{i,t}\}_{i=1}^N$ ; Approximated NTR:  $\hat{\Omega}_t$ .
Sample the set of  $N = 2^D$  points  $\tilde{\mathbf{X}}_t = \{\tilde{\mathbf{x}}_{i,t}\}_{i=1}^N$  using section strategy from Section 4.3.
for  $\tilde{\mathbf{x}}_{i,t} \in \tilde{\mathbf{X}}_t$  :
    Obtain policy  $\hat{\delta}_{i,t}$  for  $\tilde{\mathbf{x}}_{i,t}$  by solving the optimization problem using  $V_{t+1}$  as the next
    period's value function. (Terminal value function in  $t = T - 1$ )
    Compute the approximate NTR vertices  $\hat{\omega}_{i,t} = \tilde{\mathbf{x}}_{i,t} + \hat{\delta}_{i,t}$ .
end
Compute the NTR approximation:  $\hat{\Omega}_t = \{\lambda \hat{\omega}_t \mid \lambda \in (0, 1)^N, \sum_{i=1}^N \lambda_i = 1\}$ .

```

Algorithm 2. Complete Dynamic programming scheme with Gaussian process regressions and the NTR approximation.

Input : Terminal value function v_T ; time horizon T ; sample size N .
Result : Set of GP approximations of the value functions $\{v_{t-1}\}_{t=0}^{T-1}$; set of approximated NTRs $\{\hat{\Omega}_{t-1}\}_{t=0}^{T-1}$, obtained policies $\{\{\delta\}_{i=1}^{N+2^d}\}_{t=0}^{T-1}$.

Set $\mathcal{V}_T = v_T$.

for $t \in [T, \dots, 1]$:

- Approximate NTR $\hat{\Omega}_{t-1}$ (Alg. 1) using \mathcal{V}_T as the next period's value function.
- Sample N points $\mathbf{X}_{t-1} = \{\mathbf{x}_{t-1,i}\}_{i=1}^N$ using the constructed sampling scheme.
- for** $\mathbf{x}_{i,t-1} \in \mathbf{X}_{t-1}$:
 - Obtain value $\hat{v}_{i,t-1}$ and policy $\{\hat{\delta}_{i,t-1}, \hat{c}_{i,t-1}\}$ for $\mathbf{x}_{i,t-1}$ by solving the optimization problem using \mathcal{V}_t as the next period's value function.
- end**
- Define the training sets:

$$\mathcal{D}_{\text{in},t-1} = \{(\mathbf{x}_{i,t-1}, \hat{v}_{i,t-1}) \mid \mathbf{x}_{i,t-1} \in \hat{\Omega}_{t-1}\},$$

$$\mathcal{D}_{\text{out},t-1} = \{(\mathbf{x}_{i,t-1}, \hat{v}_{i,t-1}) \mid \mathbf{x}_{i,t-1} \notin \hat{\Omega}_{t-1}\}.$$

Given $\mathcal{D}_{\text{in},t-1}$ and $\mathcal{D}_{\text{out},t-1}$, approximate v_{t-1} for inside and outside of the NTR $\{G_{\text{in},t-1}, G_{\text{out},t-1}\}$ (using the respective datasets) with GPs.

Set $v_{t-1} = \{G_{\text{in},t-1}, G_{\text{out},t-1}\}$.

end

4.5 Computational stack and implementation

The solution algorithm is implemented in Python and takes advantage of a somewhat simple computational stack. following (Gaegauf, Scheidegger and Trojani 2023). The economic identities and dynamics where written using the PyTorch package, which is a machine learning library implemented in Python. This package has an auto-differentiation feature, which allows for easily implmentable gradients for the constrained optimization scheme. Furthermore this package is also directly linked with the GPyTorch package. The GPRs were implemented using the GPyTorch package, which is a Gaussian process library implemented using PyTorch. This package has multiple speedups for GPRs, such as the Lanczos Variance Estimate (LOVE), which reduces the computational burden of the GPRs. Furthermore the predictive mean can be computed using black-box matrix-matrix multiplication, which is a speedup for the predictive mean computation, skipping cholesky decompositions in favour of the conjugate gradient method for large matrices. The constrained optimizer I use is the Cyipopt package, which is a Python wrapper for the Ipopt package, which is a non-linear optimization package. This takes the automatically computed gradients and solves the optimization problem for each point in the state space. This package is used for the optimization problem for each point in the state space, and to find the optimal policy δ for each point, and likewise consumption c if this is included. The gaussian quadrature grid-points were implemented with the Tasmanian package,

which is a sparse grid package. This was taken from (Schober, Valentin and Pflüger 2022), who used this package to implement sparse adaptive grids.

Finally I implemented parallelization at two points in the code. When approximating the NTR, I can do this in parallel for each starting point in the state space. Also whenever I run the optimization scheme for a point in the state space, I can run these in parallel, as they are independent operations, as long as I do this within the same timepoint t .

4.5.1 Optimization details

When solving the optimization problem, I use a tolerance of 10^{-7} , and 1000 iterations. When approximating the NTR, I solve for each point 5 times and select the optimal solution among these. Furthermore, I multiply the starting point with a decaying factor, in the number of starts, in order to add small variance at each iteration. This is because non-linear optimization problems can be sensitive to the initial starting points, so by using multiple starts, I ensure that the best solution is found. This adds some computational overhead, but I prefer to ensure that I find the best solution.

The initial starting point is chosen within the feasible space at random, when there is no approximated NTR. The random draws are chosen to be feasible given the constraints of the problem. When I later have approximated the NTR, I use the shortest distance towards the NTR as initial guess, and multiply with a decaying factor over the number of starts. For these points I solve the optimization problem 3 times. This is because when I can leverage the knowledge of the NTR, the optimization problem is easier.

For points inside the NTR I likewise guess no trading, knowing this to be optimal a-priori. Small jitter is added to this when I use multiple starts in line with the logic for all other points.

5 Results

The theoretical framework for the dynamic portfolio choice problem with fixed and proportional transaction costs was presented in Section 3. The implementation details were covered in Section 4. The purpose of Section 5 is to present the results of the implementation, as well as the changes to the theoretical framework, when fixed costs are considered. The results are presented in the following order: First, the baseline of only proportional cost is considered. I then present the new computational scheme needed to tackle fixed costs and solve this model. Afterwards I consider the results of the fixed cost model, and how the NTR changes when fixed costs are considered. During this I present how this new method can be adapted to other cost structures. Finally, I consider the results of the model with fixed and proportional costs.

5.1 Parameters and Model Setup

For the following results I consider 3 types of parameterizations for the problem. The first is a simple case where the assets are identically distributed (i.i.d), these parameters are seen in (Cai, Judd and Xu 2013). The second is a case where the parameters are chosen to match the parameters in (Schober, Valentin and Pflüger 2022) also seen in (Gaegau, Scheidegger and Trojani 2023). This is in order to be able to draw correct comparisons between the results. Furthermore, this case showcases assets with slight variation in the mean return and a small correlation between the returns, and there is no asset which the others. The last parameterization is a modification of the first case where the correlation between the returns is large (correlation coefficient of 0.75). This parameterization clearly displays the effect of correlation on the NTR. The parameters for the three cases are displayed in Table 1.

Table 1: Parameters for portfolio models

	i.i.d Assets	Schober Parameters	High Correlation
T	6	6	6
Δt	1	1	1
k	3	5	3
γ	3.0	3.5	3.0
τ	0.5%	0.5%	0.5%
β	0.97	0.97	0.97
r	3%	4%	3%
μ^\top	(0.07, 0.07)	μ_{Schober}	(0.07, 0.07)
Σ	$\begin{bmatrix} 0.04 & 0.00 \\ 0.00 & 0.04 \end{bmatrix}$	Σ_{Schober}	$\begin{bmatrix} 0.04 & 0.03 \\ 0.03 & 0.04 \end{bmatrix}$

$$\mu_{\text{Schober}}^\top = [0.0572 \ 0.0638 \ 0.07 \ 0.0764 \ 0.0828]$$

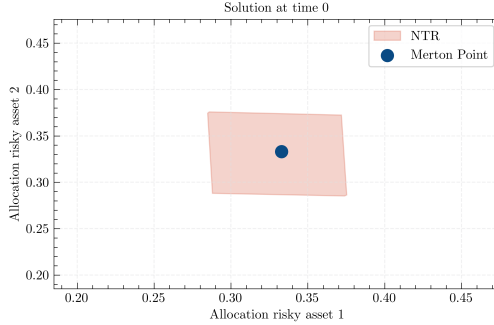
$$\Sigma_{\text{Schober}} = \begin{bmatrix} 0.0256 & 0.00576 & 0.00288 & 0.00176 & 0.00096 \\ 0.00576 & 0.0324 & 0.0090432 & 0.010692 & 0.01296 \\ 0.00288 & 0.0090432 & 0.04 & 0.0132 & 0.0168 \\ 0.00176 & 0.010692 & 0.0132 & 0.0484 & 0.02112 \\ 0.00096 & 0.01296 & 0.0168 & 0.02112 & 0.0576 \end{bmatrix}$$

5.2 Dynamic Portfolio Choice without consumption

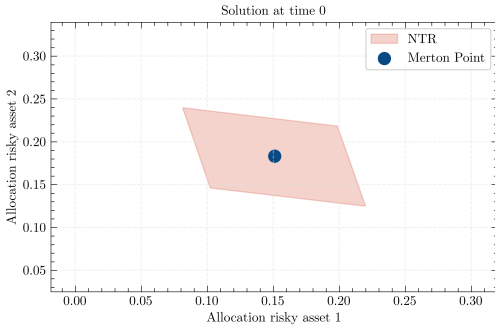
I first consider the base model with proportional transaction costs and no consumption. In the absence of consumption, the optimal portfolio is the Merton point, which I plot in every figure. I plot the No-trade region at time point 0 (initial time point) for each of the parameterizations in Figure 5.1. When using the Schober parameters I select the d

first elements of the mean vector and truncate the covariance matrix to a $d \times d$ matrix, depending on the number of assets d in the model. If I consider larger dimensions for the other parameters, I simply add more assets with the same mean and covariance structure. I solve the models for a $T = 6$ year horizon. I note that for each of the parameterizations

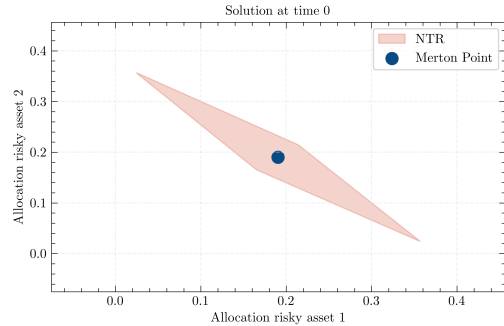
Figure 5.1: Comparison of No Trade Regions with proportional costs.



(a) No Trade Region for Independent Identically Distributed Assets.



(b) No Trade Region for Schober Parameters.



(c) No Trade Region for High Correlation.

the No-Trade region is a rectangle or parallelogram. The Merton point is located in the center of each NTR and the NTR is symmetric around the Merton point.

The i.i.d parameterization has the highest optimal asset allocations, which is due to the high returns of the risky assets. the Merton point is $(0.33, 0.33)$. The NTR is almost a perfect square, but displays slight skewness. This is numerical instability in the optimization process, and compounding value function approximations.

For the Schober parameters and the high correlation case, the No-Trade region is a parallelogram. This is due to the correlation between the returns. When some correlation is present, the No-Trade region is skewed, since some allocations that would be optimal in the absence of correlation are no longer optimal. This is because when the returns are correlated, the assets are substitutes to the degree of correlation. Large weighting in one risky asset are then only optimal, by reducing the weight in another asset, in order to diversify risk for the investor. Comparing the Schober parameters to the high correlation case, this is apparent. Likewise, if the correlation was inversed, the investor would prefer

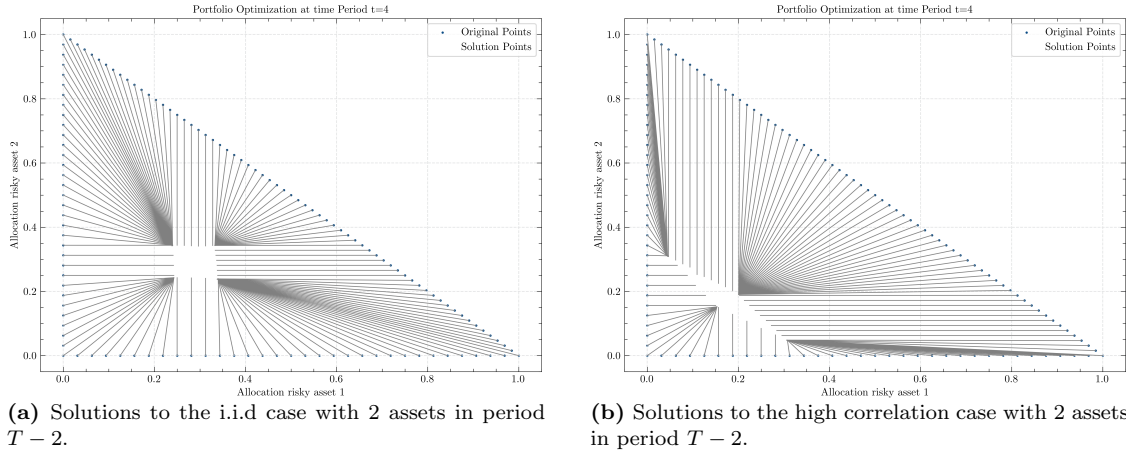
high weighting in both assets in order to hedge risk.

5.2.1 Verifying the geometric shape of the No-trade Region

Since much of the procedure for solving this problem, and approximating the NTR leverages the a-priori assumptions regarding the geometric shape of the NTR, I first want to verify that the NTR indeed has 4 vertices for the 2d case, and no more, and is a convex hull.

In order to do this, I do a small modification to the solution algorithm proposed earlier. Instead of computing vertices using 2^d predetermined points, I will instead sample a larger set of points, ($2^7 = 128$) covering the boundaries of the feasible state space. For each of these points, I then solve the optimization problem and plot the solution from allocations \mathbf{x}_t and their solutions to the problem $\hat{\omega}_t$. I do this by using my original sample scheme, and adding mid-points between points, which either sum to 1.0 or have 0.0 as allocation for one of the assets. I consider the i.i.d case and the high correlation case, with $\tau = 0.0075$ i.e 0.75%. I have increased the costs slightly in order to increase the size of the NTR. This is to ensure that points also converge towards the faces and not only the vertices by extending the length of the faces. This is akin to the green regions in Figure 4.3. Otherwise I would need more points on a finer grid. I plot the solutions for next to last period with investment decisions $T - 2$. The solutions are plotted below.

Figure 5.2: Verifying the assumptions of the NTR in two dimensions.



I find that the assumptions regarding the NTR are indeed correct in the two dimensional example, I constructed. Furthermore, this verifies that the assumptions also hold for correlated returns, as conjectured by (Liu 2004) and found by (Cai, Judd and Xu 2013). Furthermore, these plots also nicely confirm that the optimization process as a whole works as intended and provide an intuitive understanding of the NTR. Further verification in higher dimensions are not considered. First of all (Liu 2004) confirm this formally in

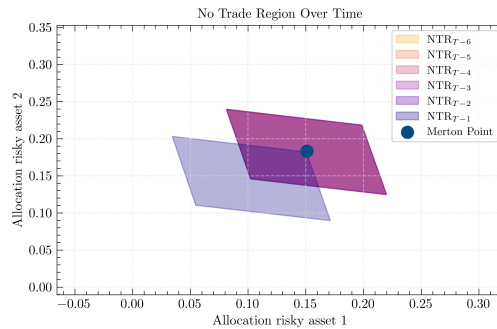
larger dimensions for the case of uncorrelated returns and the intuition regarding the NTR does not change when dimensionality is increased.

5.2.2 Investigating the No-Trade Region

I now look at the No-Trade region for the base model with proportional transaction costs and no consumption in more detail. Specifically I look at how the region behaves over the entire investment horizon $[0, T - 1]$, and how the region changes with different transaction cost levels. I choose to look at the model with the Schober parameters as this is a mixture of the other two parameterizations.

I first solve the model for the Schober parameters, and plot the NTR for each time point in the investment horizon.

Figure 5.3: No Trade Region for Schober Parameters over Time.

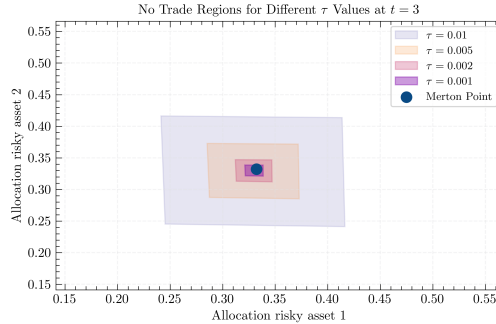


The No-Trade region is plotted for the Schober parameters over the entire investment horizon $[0, T - 1]$. For time points $t \in [0, T - 2]$ the NTRs overlap.

I note that at the last time point $t = T - 1$ the NTR moves away from the Merton point towards the origin, and the Merton point is then at the upper right corner of the NTR. For all other time periods the NTR is the same, and the Merton point is in the center. This is consistent with behaviour found by (Cai, Judd and Xu 2013; Gaegau, Scheidegger and Trojani 2023), and might suggest that I only require solutions for two periods, $T - 1$ and $T - 2$ in order to effectively cover the NTR for all periods. I can therefore use the solution for $T - 2$, which is higher quality than $t = 0$, due to numerical instabilities in the optimization process, and effectively cover the NTR for all time points.

I now investigate how the No-Trade region changes with different transaction cost levels. I do this for the i.i.d. parameters, and plot the NTR for different values of τ in Figure 5.4 for $\tau \in \{0.01, 0.005, 0.002, 0.001\}$. When the transaction costs are increases the NTR increases as well and vice-versa. I note that for low enough transaction costs, the NTR shrinks towards the Merton point. However, when transaction costs are low enough, the Merton point is not in the exact center, which might signify that at low enough values,

Figure 5.4: No Trade Region for the i.i.d Parameters with different values of τ .

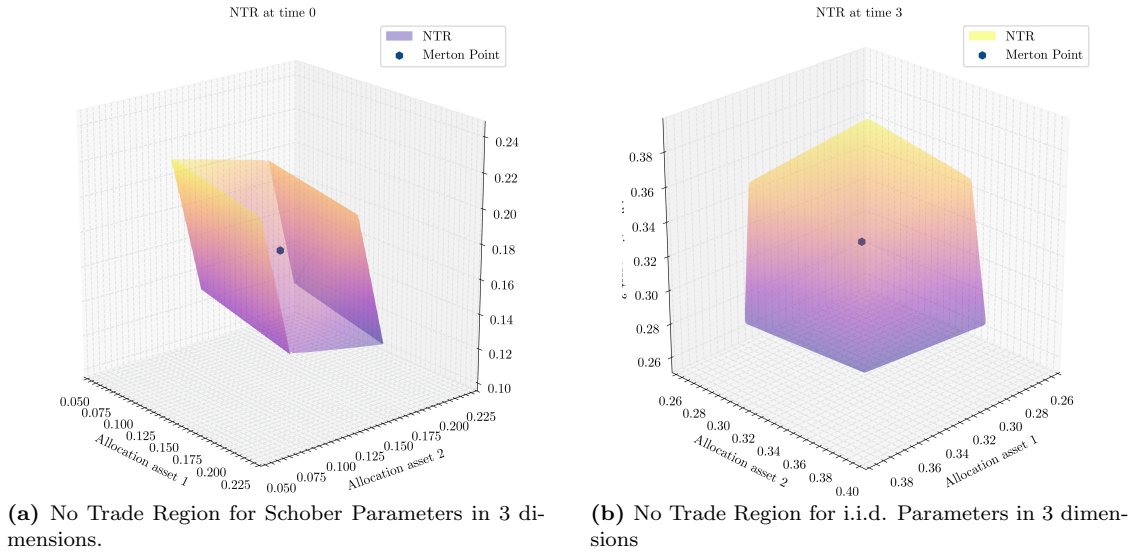


some numerical instabilities from the minimizer and function approximation using GPR, might be present.

5.2.3 Increasing the dimensionality of the model

I now increase the dimensionality of the model to $D = 3$ and look at the No-Trade region for the Schober parameters and for the i.i.d parameters.

Figure 5.5: Comparison of No Trade Regions with three risky assets.



I plot the NTR with open faces, however the actual NTR has all the faces closed, and is a convex hull. I plot for time period $T - 3$. This choice is arbitrary. Note, that the i.i.d NTR looks like a skewed cube, whereas this was a perfect square in the 2 dimensional case.

Looking at the points forming the convex hull that is the NTR, it is clear that the NTR is restricted by the no-borrowing constraint. The border points, which would otherwise

form the perfect cube, would outside the feasible space if borrowing was possible, and is then projected back into the feasible space, hence the skewness. The Merton point for the i.i.d case with three assets is $(0.33, 0.33, 0.33)$, and the total risky investment portfolio is 99% of wealth, hence the Merton point is close to the border of the feasible space. Thus, when the risky returns outweigh the risk-free return, to such a degree that the Merton point moves towards the boundary of the feasible space, cube like shapes are no longer possible. In the case of two risky assets, this is akin to the NTR being close to the budget line, and the NTR would then form a triangle.

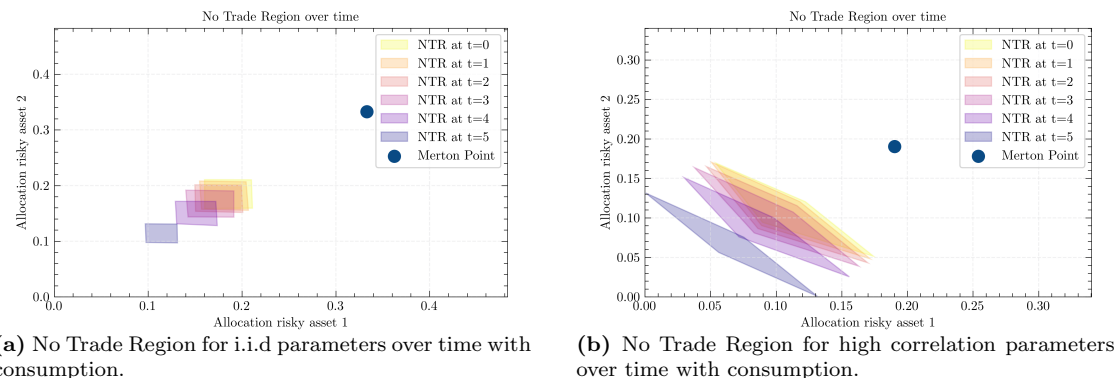
This is clear when compared to the Schober parameters, where the Merton point is in the center of the NTR, and the NTR is a skewed cube well within the feasible space. The Merton point in this case suggests lower portfolio allocations to the risky assets, and hence the NTR is not restricted by the no-trading and no-borrowing constraints. The NTR behaves similar to the 2d case, and the intuition regarding the NTR is the same.

Furthermore the NTR behaves similar to the 2d case, and is only considerably different in period $T - 1$, compared to periods $T - 2, T - 3$ and so forth.

5.3 Dynamic Portfolio Choice with consumption

I now consider the base model with proportional transaction costs which now includes consumption of a non-durable good. This adds an extra decision variable which needs to be solved for, and consumption now adds immediate utility to the investor in each period.

Figure 5.6: Comparison of No Trade Regions over time with consumption.



The No-Trade regions are plotted over the entire investment horizon $[0, T - 1]$.

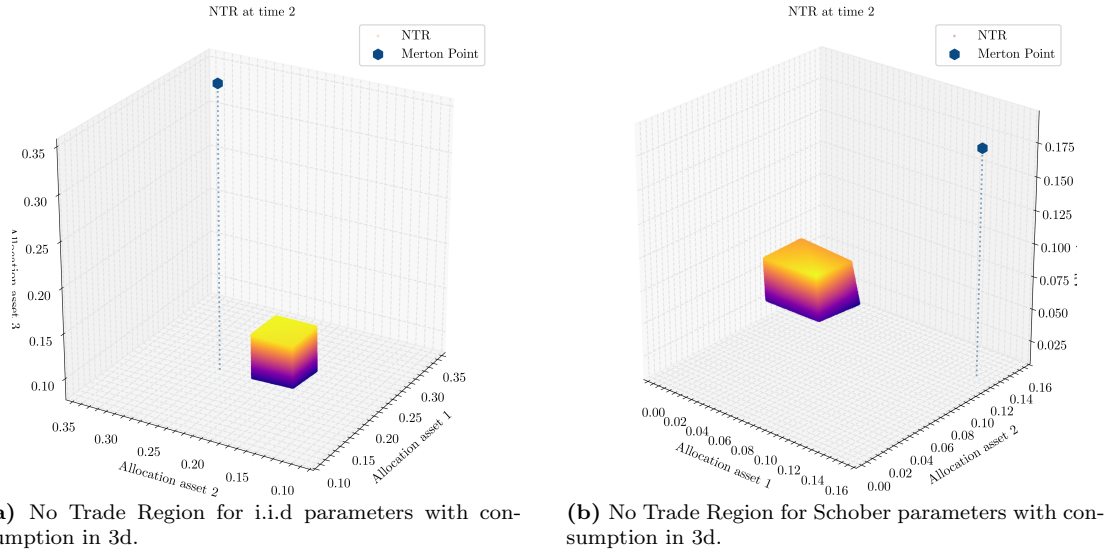
Note, that when consumption is included, the NTR no longer encapsulates the Merton point at any time point. If the Merton point is scaled to the wealth after consumption, $x_t^{\text{Merton}} \cdot (1 - c_t^*)$ then the Merton point is encapsulated by the NTR.

Furthermore, the NTR now moves over time towards the origin as opposed to the case without consumption, where the NTR was static for all time points except the next to last period (last period with trading decisions). Hence, the NTR is now no longer sufficiently described by solutions to $T - 1$ and $T - 2$ as the optimal consumption decision changes over time, moving the NTR towards the origin, as $t \rightarrow 0$.

The shifts of the NTR diminish as $t \rightarrow T$, as I note that the largest movement occurs from $t = T - 1$ to $t = T - 2$. This is because the consumption decision increases exponentially over time.

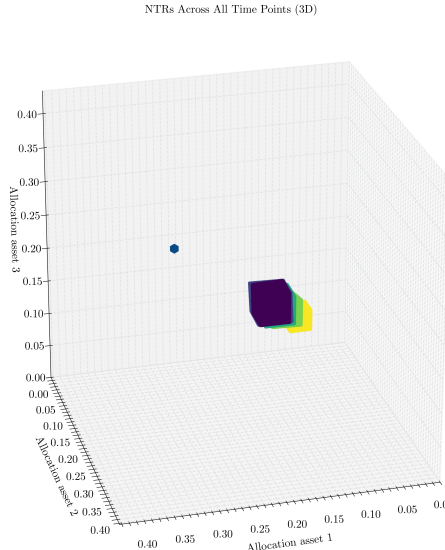
This behaviour is consistent in higher dimensions, and with results found by (Gaegauf, Scheidegger and Trojani 2023). Below are plots of the NTR for two different parameterizations of the model, with three assets, at a singular time point.

Figure 5.7: No trade regions with consumption in multiple dimensions, singular time period



I can similar to the two asset case, plot the NTR over the entire investment horizon, as seen in Figure 5.8a. Once again, I note that the NTR moves towards the Merton point as $t \rightarrow T$, but never encapsulates the Merton Point. Likewise, the movements of the NTR diminish as $t \rightarrow 0$, since the change in consumption decision between periods diminishes as $t \rightarrow 0$.

Figure 5.8: No trade regions with consumption in multiple dimensions entire horizon



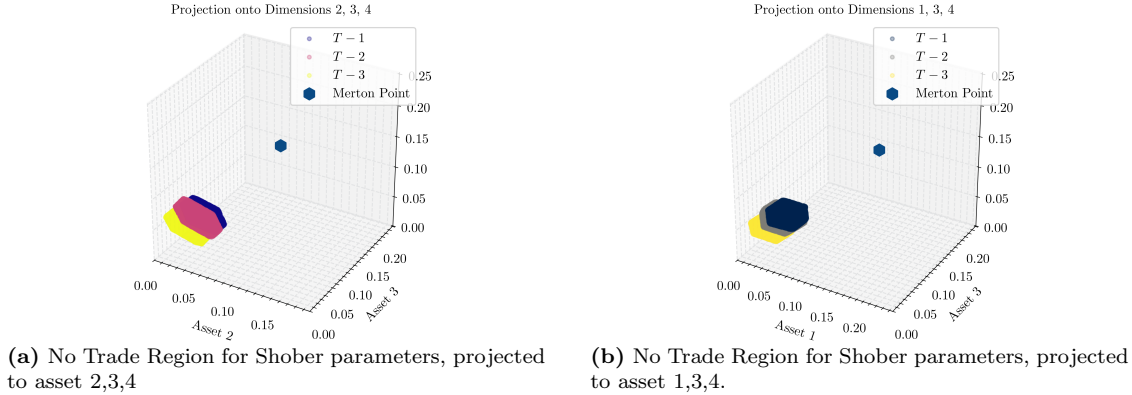
(a) NTR for 3 assets with i.i.d parameters over time with consumption.

5.3.1 Increasing the dimensionality of the model further

I now look at increasing the dimensionality of the model even further. This moves the solutions of the model to higher dimensional spaces, which have well defined mathematical properties. Illustrations will be projected to three dimensions, as the model is not easily visualized in higher dimensions. I solve the model with the Schober parameters for $d = 4$ assets with consumption. This increases the complexity of the model, and the NTR is now a hyper-cube, however solutions remain feasible, despite the algorithm running on a laptop computer. For the $d = 4$ case, the Merton point is $(0.1448, 0.0971, 0.1317, 0.1522)$ which suggests a total risky investment portfolio of 52.58% of wealth. I use $60 \cdot D = 240$ generated points and their respective solutions to train the GP in each iteration. Approximating the NTR by itself now takes considerably longer¹³ than the previous cases, and the NTR is projected to three dimensions. and larger dimensions $D > 4$ are therefore not in the scope of this paper, as the computational power required is too large for me to handle . However, solving the 4 risky asset porfolio, on a personal laptop, remains a computational feat, as previous studies (Cai, Judd and Xu 2013; Schober, Valentin and Pflüger 2022) relied on super computers to solve the model. (Gaegau, Scheidegger and Trojani 2023) makes no mention of the computational setup, and a direct comparison to the results is therefore dissapointingly not possible. The NTR is plotted below, and each vertice for $T - 1$ and $T - 2$ can be found in Appendix B

¹³Solving for three periods took 180 minutes.

Figure 5.9: No trade regions for Shober parameters with consumption, four assets projected to three dimensions.



5.4 Dynamic Portfolio Choice with fixed costs

I now consider the base model with fixed transaction costs and no consumption. From (Dybvig and Pezzo 2020), I know that the NTR is no longer rectangular when we only consider fixed costs, but instead circular with the Merton point in the middle when there is no consumption in the model. This poses a problem for my current sampling scheme, which leverages my predetermined knowledge of the geometric shape of the NTR. As I noted in Section 4.3, in order to effectively sample points for the NTR approximation, given the framework for the proportional cost case, I now need to sample points, such that when they hit the NTR these points are evenly distributed on the sphere, in order to approximate the NTR correctly. However this is still not sufficient as the fixed costs pose further problems for the solution algorithm by (Gaegau, Scheidegger and Trojani 2023). In order to see this a little intuition is needed.

5.4.1 Generating a new solution algorithm for the fixed cost case

Transaction costs no longer scale in the fixed case, but are treated as a *sunk cost*, the moment the decision to trade is made. Hence, if trading is optimal the investor will trade to the optimal point, and if trading is sub-optimal then no trading will occur. The problem is therefore first of all a trading decision problem. If trading is optimal, then the investor will trade to the Merton point when no consumption is present, as this is the optimal point.

This is in stark contrast to the proportional case, where the trading trajectory from outside the NTR was to the border of the NTR, and the NTR approximation could be done by sampling points on the border of the feasible space.

Now, any point sampled outside the NTR trades to the Merton point, and I need to construct a new strategy, in order to efficiently construct the NTR, as no new information

is gained by sampling multiple points outside the NTR.

Furthermore, the transaction cost function is now an indicator function, depending on a threshold, i.e $\sum_{i=1}^k \delta_{i,t}^+ + \delta_{i,t}^- > 0$. This is non-differentiable at the kink, $\sum_{i=1}^k \delta_{i,t}^+ + \delta_{i,t}^- = 0$ which is a critical point (the trading decision boundary), that I have to deal with in order to solve the optimization problem.

I therefore split the optimization process into two parts. I evaluate the objective function (value function), *conditional* on no trading ($\boldsymbol{\delta}_t = \mathbf{0}$) and *conditional* on trading ($\boldsymbol{\delta}_t \neq \mathbf{0}$). Since there is no consumption decision then the no-trading decision is trivial, whereas I still optimize the trading decision conditional on trading occurring in order to maximize expected utility.

By splitting the optimization process, I can avoid the the non-differentiable edge case, and the gradients are trivial for the optimizer. I then evaluate the value function for the no-trading decision, and the trading decision, and choose the decision which maximizes the value function. Furthermore when splitting the problem by the trading decision, the optimization problem is convex once again, as per (Dybvig and Pezzo 2020). Hence the issues mentioned in Section 4.3 are no longer present.

I now consider the base model with fixed transaction costs, and no consumption. I use the simple i.i.d parameterization, with two assets and solve the optimization problem for the next to last period $T - 1$ over an evenly spaced grid of points. I do this in order to verify that the solution algorithm works as intended, and that the NTR is circular as expected, conflicting with my prior assumptions for the proportional case.

I set the fixed costs to 0.005% of the investors total wealth at any time point and solve at a very fine grid of points, in order to approximate the NTR correctly. I find that the NTR is circular as expected, and that the new solution algorithm works as intended.

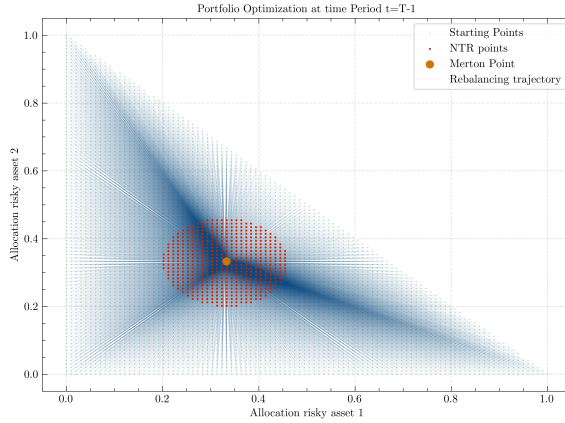
I therefore proceed with generating a strategy for dealing with fixed costs, which can leverage my new found knowledge of the NTR.

5.4.2 Constructing a new sampling scheme and approximation method for the NTR

Noting that for each point outside the NTR, the investor will trade to the same optimal point, since the cost of trading is a *sunk cost*, I can select a single starting point at the origin and solve for the optimal trading decision. If the optimal decision is to trade, then I immediately know the center of the NTR and now only need the radius to construct the NTR. This holds for any dimensionality of the model, as any circle/sphere/hypersphere can be defined by the center point and the radius.

I find the radius, by moving towards one of the boundary starting points, from the center of the NTR, solving the optimization problem for each point, and noting at which point that trading occurs (return to the center).

Figure 5.10: Grid solution to the i.i.d case with fixed costs, two assets in period $T - 1$.



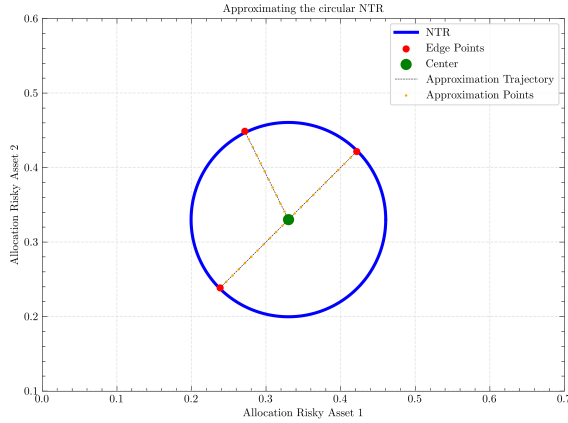
The optimization scheme ran with 5044 evenly spaced grid points. The points are plotted in the feasible space, and the NTR is the convex hull of these points.

By using a bisection method¹⁴, I find the border of the NTR with a tolerance of $5 \cdot 10^{-7}$, which is a tolerance equal to 0.00005% of the total wealth of the investor. I solve for multiple directions from the center, and choose the largest radius. This is because the circle might be truncated along the borders of the feasible space if the NTR is close to either of the axis or the budget constraint (no borrowing/shorting). Furthermore, by selecting directions in evenly spaced angles around the center, I ensure that one of the directions of trading, must hit the border as long as the NTR does not cover the entire feasible space. For the latter case, the algorithm would never find a center point, and the solution is trivial any how.

This optimization process can be seen in Figure 5.10. I start from a blue point and rebalance to the Merton point. Then turn to Figure 5.11, I move along a straight line in the direction of a starting point outwards and solve. If no trading occurs the point is in the NTR. If trading occurs then the point is outside the NTR, and I move backwards towards the center, and solve again. This is repeated for each trading direction. The figure below displays this specific part of the algorithm.

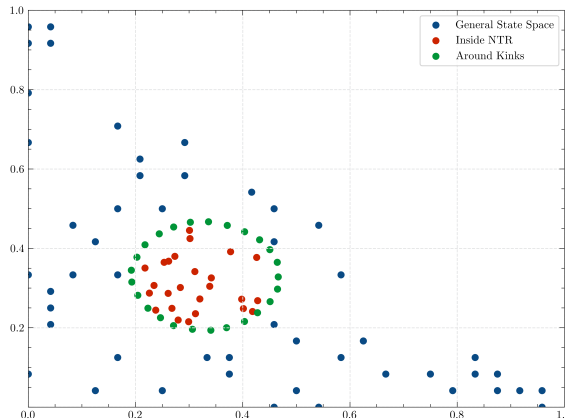
¹⁴Which is simple to implement since we only consider allocations along the straight line from some angle outwards from the center of the NTR.

Figure 5.11: Two dimensional approximation algorithm for the fixed cost NTR with no correlation.



I also need to consider the sampling strategy for my GPR-related training points. As I mentioned previously, I need to sample three types of points. Points within the NTR, points outside the NTR, and points near the border the NTR. The last points were previously kink points, when the NTR had followed assumptions 1 and 2. For the circular case however, there are no kinks. The previous sampling strategy is otherwise easily applicable to the circular case, but for the border points, I change the strategy slightly. I sample evenly spaced points (defined by their relative angle to the center point) on the border of the approximated NTR, and add random positive noise to ensure these are outside the NTR. This effectively covers the entire circle, and I can now leverage a low amount of training points for the GPR as for the proportional cost case.

Figure 5.12: Sampling strategy for the fixed cost NTR, with no consumption or correlation.

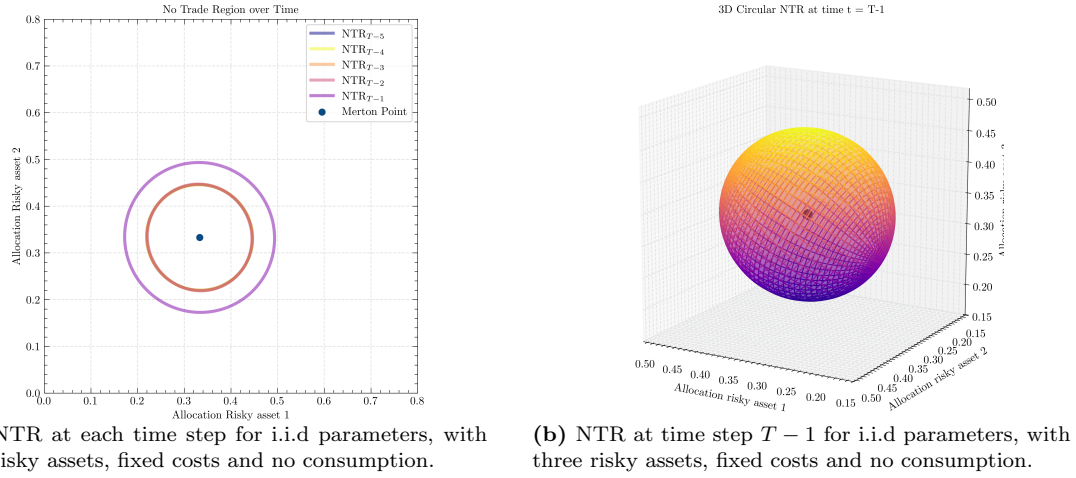


this sample strategy uses the same number of points as the schematic for the proportional cost sampling strategy

5.4.3 Fixed costs No-Trade Region without correlation

I now employ the mentioned algorithm, and solve the fixed cost case for the i.i.d parameters, with two assets, and no consumption. I solve the problem with the i.i.d parameters and a fixed cost of 0.075% of the investors total wealth at any time point. I consider an investment horizon of $T = 5$.

Figure 5.13: Fixed cost No-Trade Regions with i.i.d assets.



Sample points for the GPR used 210 points. Fixed costs at 0.075% of total wealth.

For the plot with two risky assets, I note that the NTR displays two distinct regions, one for $t = T - 1$ and one for $t < T - 1$. At the last period, the NTR is larger and the fixed costs affect the trading decision moreso than for periods $t < T - 1$. The Merton point is now in the center of the NTR, and the NTR is circular as expected.

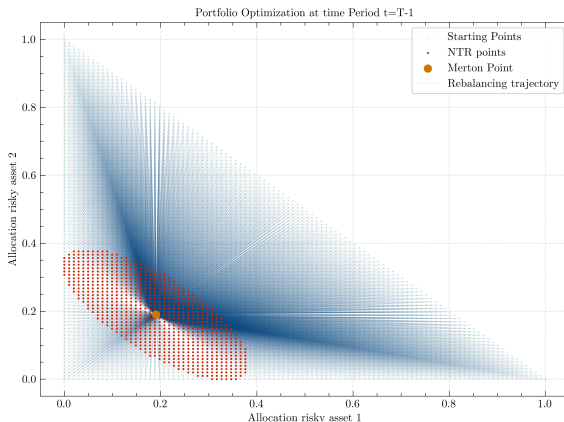
At time step $T - 1$ the radius is 0.16 whereas for time step $T - 4$ (0) the radius is 0.11. Hence, when fixed costs are considered only two periods need to be solved for, in order to approximate the NTR over the entire investment horizon. Any more solutions will only add to the approximation error, and the true NTR will not change significantly. I likewise solve the model for $D = 3$. I note for the three risky assets case that the NTR is now a sphere, which is to be expected, as the NTR is extended to higher dimensions. In order to approximate the higher order NTRs, I use a similar fitting scheme as in Figure 5.11. This is displayed in Figure C.1 located in Appendix C. The fixed costs problem can likewise be solved in higher dimensions, however since this poses no changes to the proposed solution methods, I do not consider this further, and continue to the correlated case, in order to generate a more general fixed cost solution.

5.5 Dynamic Portfolio Choice with fixed costs and correlation

I now solve the model for correlated returns, that is, I solve for the Schober parameterization and for the high correlation parameterization. I set the fixed costs to 0.005% of the investors total wealth at any time point and consider an investment horizon of $T = 5$. For the proportional cost case, when asset returns were correlated, the square was shifted into a parallelogram shape, and I expect the same to happen for the fixed cost case, shifting the circle into an ellipse. I first solve for two assets for the high correlation case, as this parameterization should have the most pronounced effect on the geometric shape of the NTR. Furthermore I want to verify that the NTR solution, once again, is defined by two distinct regions, one for $t = T - 1$ and one for $t < T - 1$, as noted in Figure 5.13a.

I first verify the shape of the NTR for the high correlation case by solving over a fine grid as previously mentioned.

Figure 5.14: Grid solution to the high correlation case with fixed costs and two assets in period $T - 1$.



The optimization scheme ran with 5253 evenly spaced grid points. The points are plotted in the feasible space, and the NTR is the convex hull of these points. Fixed costs at 0.0005.

I note from Figure 5.14 that the NTR is now an ellipse, as expected. This new shape is due to the correlation between the returns, and the NTR is now skewed, as the returns are correlated. This is because the assets are now substitutes to some degree given by their positive correlation. I then need to reformulate the solution algorithm for this case, as the NTR is no longer circular, and the solution algorithm for the fixed costs case with i.i.d assets is no longer applicable, since an ellipse is not defined by a center point and a radius. Thus, I need to adapt the solution algorithm, in order to approximate the NTR correctly.

An ellipse in two dimensions is defined by its *foci*. For any point on the ellipse, the sum of the distances to the foci is constant. The ellipse has a major diameter (major

axis) and a minor diameter (minor axis), respectively the longest and shortest distance between two points on the ellipse (Ivanov 2020). Given a center point and enough points on the border of the ellipse (which may be noisy) I can approximate the ellipse by a least squares algorithm (Gander, Golub and Streb 1994). This requires enough points in order to solve the the problem sufficiently.

For two dimensions the minimum required points are 5 points with no three points collinear. For higher dimensions the required points are $d(d + 3)/2$ points, however otherwise the same procedure can be applied (Bertoni 2010).

I modify the solution algorithm in the following manner. I solve the optimization problem for a single point outside the NTR, and find the optimal trading decision towards the center¹⁵. I then sample $d(d+3)/2 + 2^d + d + 1$ points, on the borders of the NTR. The 2^d points are the border points used for the square NTR sampling scheme. I then add $d(d + 3)/2 + d + 1$ random points, which are still on the border of the feasible space, by drawing random points on the border¹⁶. This should leave me with enough points which are not collinear, to approximate the ellipse. I then proceed with the bisection algorithm as previously mentioned, until I for each direction from the center, find the border point of the NTR.

I then apply the least squares algorithm and solve for the parametric equation of the ellipse (Gander, Golub and Streb 1994; Bertoni 2010). This method has the advantage that I can still solve for the ellipse using relatively few points, and these points need not cover the ellipse evenly, as the least squares algorithm will find the best fit ellipse for the points given¹⁷. The rest of the circular algorithms can be used as before. Hence the ellipse NTR is slightly more complex, given the fitting scheme and points required, but the rest of the solution algorithm is the same.

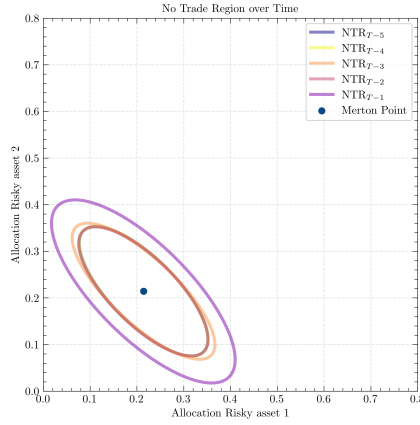
I do a slight modification to the high correlation μ vector in order to move the Merton point and make space for the resulting NTR. The new mean asset return is now $\mu = 0.075$ for each asset. This moves the Merton point to $(0.2143, 0.2143)$ from the previous $(0.1905, 0.1905)$. The solution for each time point is plotted below: As expected, the NTR adjusts in the same manner as for the i.i.d case, and shrinks from period $T - 1$ to $T - 2$. Following this the NTR is constant, with some compounding approximation error across periods. Therefore, in order to approximate the NTR over the entire investment horizon, only two periods need to be solved for, as the NTR does not change significantly over time. Also note that the NTR still displays the same logic as for proportional costs, in regard to the substitutability of the assets, but slightly larger weighting of the risky

¹⁵I do this for a few points in order to ensure that the point is outside the unknown NTR. However, a singular point is all that is needed. For example full investment into one of the risky assets, will most likely fall outside the NTR.

¹⁶I constrain these points so they are sufficiently distanced from my previously sampled points. This ensures that the resulting directions from the center are unique, and border points are not identical.

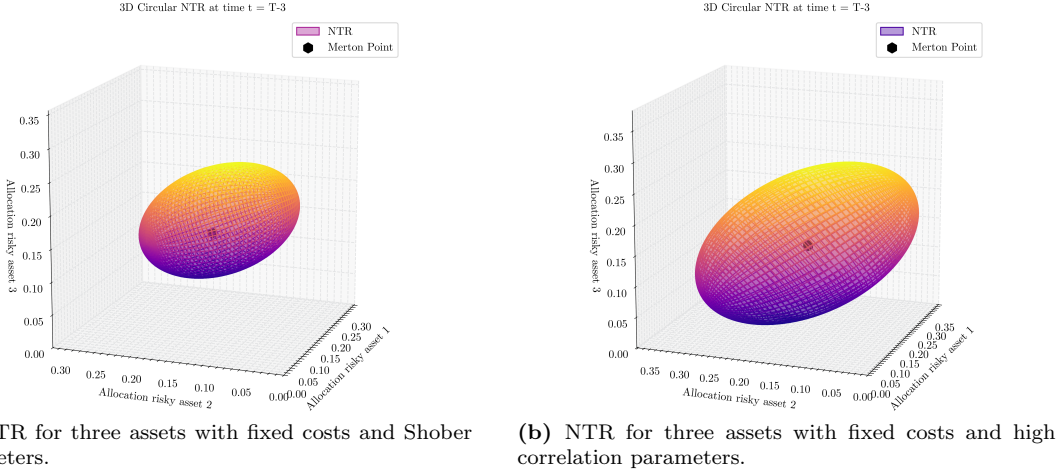
¹⁷This is also why small noise is not an issue.

Figure 5.15: NTR for two assets with fixed costs and high correlation parameters.



assets is now preferred, compared to the case for proportional costs. I now increase the dimensionality of the model to $d = 3$ and look at the No-Trade region for the Schober parameters and for the high correlation parameters. The resulting NTRs are plotted below.

Figure 5.16: Three asset No-Trade Regions with fixed costs and correlation



The No-Trade regions are plotted at time $T - 3$ which for 5 periods is $t = 2$.

The resulting NTRs are now ellipsoids, and the intuition from the two dimensional case carries over to the three dimensional case. The shape is now similar to an american football, and the high correlation case has more pronounced skewness as expected due to substitutability between the assets.

5.6 Adjusting the algorithm to new cost structures or assets

Given the methods I used, to adjust the original solution algorithm to the fixed cost case, I can now propose a general plan for adapting my framework to new cost structures. The framework applied followed these steps:

1. Solve the optimization problem over a fine grid, in order to verify the shape of the NTR.
2. Construct a new approximation scheme for the NTR given the new shape.
3. Construct a new sampling scheme for the GPR in order to approximate the NTR.
Points near the NTR and its vertices, if it has any are of high importance.
4. Solve the dynamic portfolio choice problem, and approximate the NTR over the entire investment horizon.

Given this framework, the solution algorithm can be adapted to a wide range of cost structures, not considered. These cost functions could be: Quadratic costs, asset specific proportional costs, asset specific fixed costs and combinations of these. Price impact could likewise also be considered. These costs structures are solved in the static case by (Dybvig and Pezzo 2020).

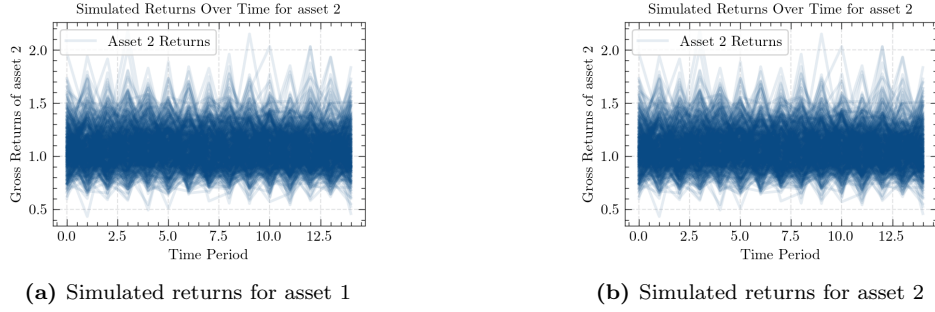
This method of adapting the solution algorithm can also be applied to new asset structures. I consider this proposed framework to be a contribution to the literature, as it allows for much future research to be conducted.

5.7 Portfolio simulations

I now simulate actual investor behavior, given the NTR and the optimal trading decisions and consumption decisions. I also simulate a competing strategy, which is to trade with no regard to transaction costs¹⁸, and consume the optimal amount of wealth in each period. This is done in order to compare strategies which take transaction costs into account when rebalancing and strategies which do not. For each simulation I draw 499 random paths for the risky asset returns, and simulate my investor, according to the chosen rebalancing strategy and consumption decisions. I simulate $T = 15$ time periods. Simulated returns are plotted below:

¹⁸This is to the Merton point when consumption is not included. When consumption is included this is to the Merton point, multiplied by $(1 - c_t^*)$.

Figure 5.17: Simulated returns for the two assets over time.



5.7.1 Portfolio simulations with fixed costs

I solve the portfolio problem for the high correlation parameters for two assets and fixed costs at $fc = 0.0005$ i.e 0.05%. I solve the model for $T = 15$ time periods. I then draw 499 random paths for the risky asset returns, and simulate my investor, according to the chosen rebalancing strategy and consumption decisions. This is done by:

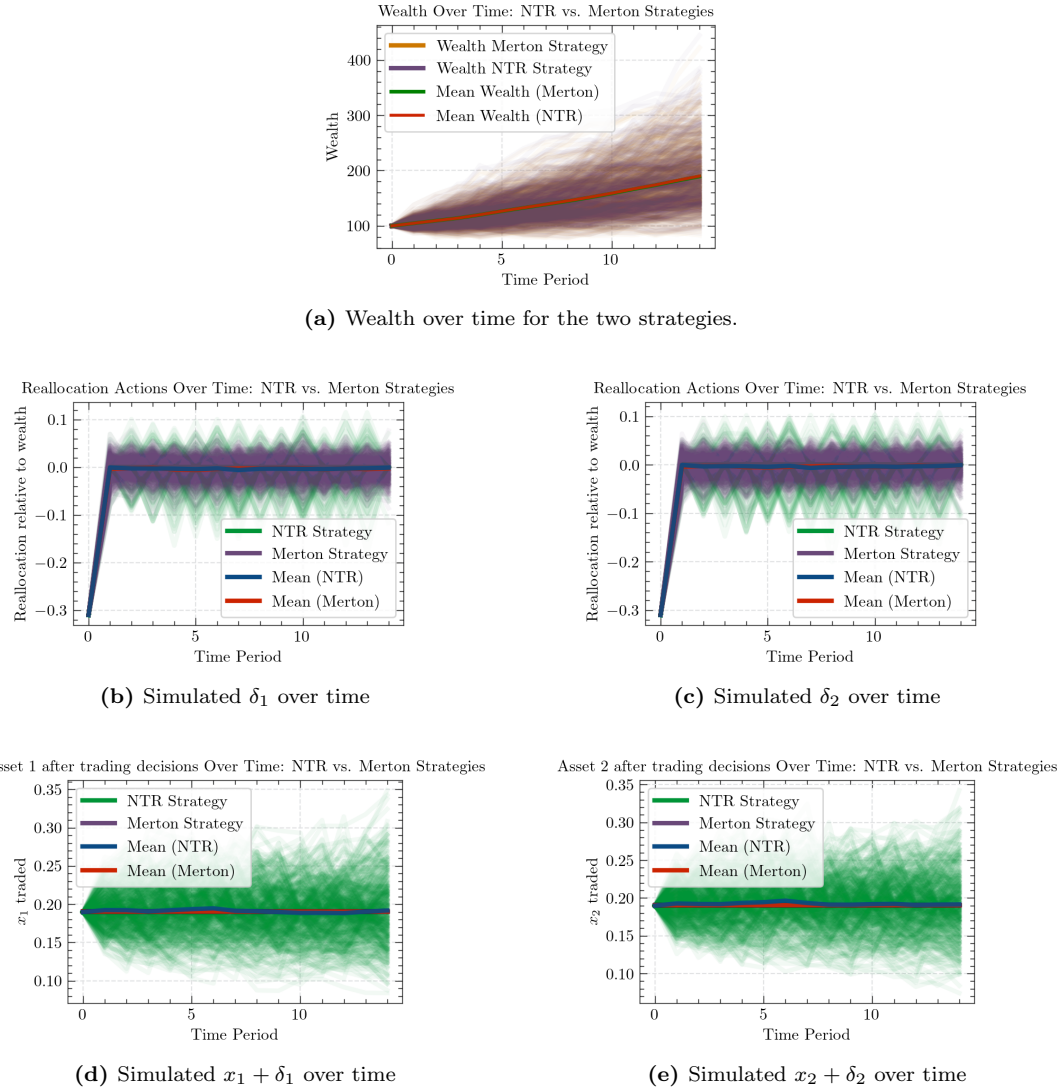
1. Setting initial allocations¹⁹ $\mathbf{x}_{t=0} = (0.5, 0.5)$ and initial wealth at $W_{t=0} = 100$
2. For each time period t from 0 to $T - 1$ do:
 - (a) Solve the optimization problem for the given time period, and find δ_t^*, c_t^* (b_t^* residual)
 - (b) Use drawn asset returns and state dynamics to compute next periods states
 - (c) repeat until $t = T - 1$

For the rebalancing strategy which trades to the Merton point, I set $fc = 0.0$ when solving for the optimal trading and consumption decision. However, fc is non-zero in the actual state dynamics. This is equivalent to not incorporating transaction costs in the rebalancing strategy. For the NTR strategy, I set $fc = 0.0005$ when solving for the optimal trading and consumption decision, as in the actual state dynamics.

I first simulate the model with no consumption, and plot relevant variables over time for each simulation, and the mean of the simulations. Figure 5.18 displays the simulated variables over time for the fixed cost case. I track the total wealth of the investor, the trading decisions, and the new allocations after trading but before they are subject to returns. This is to display the strategies before random shocks (returns). I note firstly that the NTR strategy outperforms the no transaction cost strategy, as expected. The final mean total wealth of the NTR strategy is $W_{T-1} = 190.039$, whereas the no transaction cost strategy has a final mean total wealth of $W_{T-1} = 189.289$. Thus, the performance is negligibly better for the NTR strategy.

¹⁹The choice of starting allocation is somewhat arbitrary. I choose a naive 50% split.

Figure 5.18: Simulated variables over time for the fixed cost case.



I note from the allocations after trade, that the NTR strategy contains many different allocations. These are allocations which are within the NTR, and the investor does not trade, which would otherwise be to the Merton point. This can also be seen in the plots of the δ variables. For the Merton strategy, there is only one asset allocation combination which is traded to, as to be expected.

For the NTR strategy I see that trades are larger, as this only occurs sufficiently far from the Merton point. Trades are also less frequent, which is due to the the NTR. Trades are generally smaller and more frequent for the Merton point strategy, as the investor trades to the Merton point, and the Merton point is close to the border of the NTR.

5.8 Dynamic Portfolio Choice with fixed and proportional costs

I now consider the model with both fixed and proportional transaction costs and no consumption. I first solve the model with no prior knowledge of the geometric shape of the NTR, in order to verify the shape of the NTR and the solution algorithm.

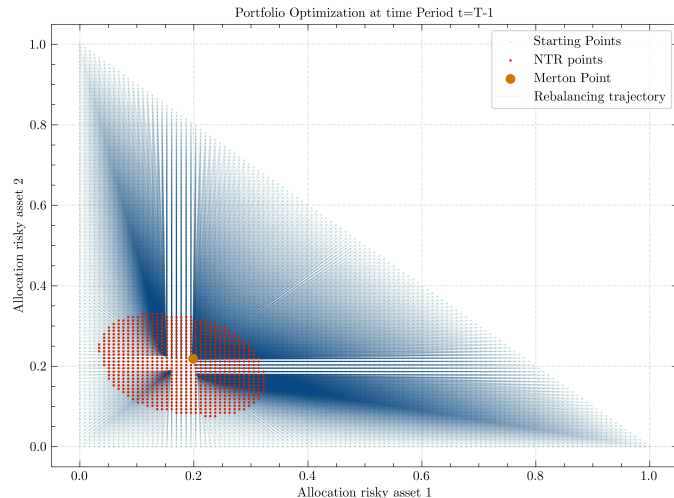
(Dybvig and Pezzo 2020) solve this in the static case, with asset specific costs, and find a hexagonal shape with an inner and outer NTR. I expect something similar to happen in the dynamic case, however whether the lines connecting the vertices are straight or not is unknown. The hexagonal shape found by (Dybvig and Pezzo 2020), seems to stem from asset specific costs, and not from the combination.

I would therefore expect an inner and outer NTR, each stemming from each type of transaction cost. I consider the Schober parameters and solve for the next to last period $T - 1$ with 2 assets. However, since the Merton point is close to the origin, and the borders of the feasible space, I add 0.005 to the mean asset return of each asset, in order to move the Merton point away from the borders. This moves the Merton point from (0.1508, 0.1831) to (0.1986, 0.2187).

I set the fixed costs to $fc = 0.0003$, which is 0.03% of the investors total wealth at any time point, and the proportional costs at 0.002, i.e 0.2% of the traded amount of wealth in each asset.

I follow my procedure and solve over a fine grid of points in order to figure out the shape of the resulting NTR.

Figure 5.19: Grid solution for two assets with fixed and proportional costs and Schober parameters.



The optimization scheme ran with 7140 evenly spaced grid points.

The figure displays the crude solution method, i.e the entirely grid based method, of the proportional and fixed cost NTR. The resulting trade decisions and NTR are a mixture

of the findings with either proportional or fixed costs, however the NTR is not a hexagon. The hexagonal shape found in (Dybvig and Pezzo 2020) does indeed seem to stem from the asset specific costs.

Instead the NTR now consists of two distinct shapes. The red points concern the ellipsoid, resulting from the fixed costs. For these points, the decision to trade is determined by the fixed cost, and the investor does not trade at all given the costs. This shape has some relation to the findings of (Liu 2004), as an inner and outer NTR is found, however the shape is not two squares, and is therefore different from the findings of (Liu 2004), but in line with findings of (Dybvig and Pezzo 2020).

When trading is optimal, the investor trades to the boundary of the proportional cost NTR, which has a parallelogram shape, and is inside the ellipsoid NTR. Optimal trading occurs to the vertices of this, and the Merton Point is at the right most border of the NTR, as previously seen in solutions to period $T - 1$ for proportional costs. Note that it is therefore no longer in the center of the ellipsoid, as for the case of only fixed costs. Hence while the ellipsoid stems from the fixed costs, the position of the ellipsoid is connected to the proportional costs, and the center of the proportional cost NTR is the center of the ellipsoid.

I propose, that for specific fractions of fixed cost and proportional cost, the vertices of the proportional cost NTR, will be on the border of the fixed cost NTR and the NTR will be a combination of the two shapes.

The NTR would in this case have vertices, which are the intersection of the two NTRs, but these would be connected by curved lines, from the fixed cost ellipsoid.

Whether the proportional NTR or the fixed cost NTR forms the outer most NTR is unknown a priori, without further investigation.

Interestingly, the proportional cost part of the NTR, is inside the fixed cost NTR, despite the proportional cost being higher than the fixed cost.

It is therefore not trivial to determine parameterizations where the two NTRs would form a cohesive shape, and this is left for future research.

As the optimal trades are no longer trivial in any manner, when the location of the NTR, its skewness and angles are all unknown a new tailored solution algorithm would be needed to effectively cover this case.

The case of the proportional cost NTR being the outermost NTR at any point is identical to the case of only proportional costs, and is therefore easily solvable with the previously mentioned solution algorithm. In this case fixed costs are of no concern.

However when the reverse case is true, as in Figure 5.19 the solution algorithm is not applicable, and a new solution algorithm is needed.

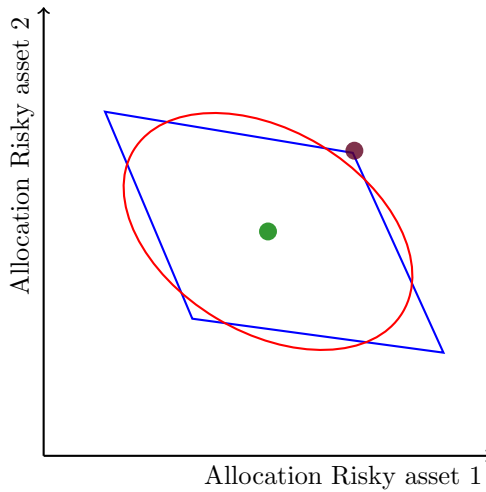
Solutions return the vertices of the inner NTR, and the bisection algorithm is therefore not immediately applicable either.

Firstly the center point would have to be found, as the center of the inner NTR,

and the border points would have to be found, in order to approximate the NTR. Then the bisection algorithm could be applied to find the border, and then I would have to determine the final NTR.

I note that this is even more complex. Furthermore, an even worse outcome can occur, if the proportional cost NTR is sometimes the outermost NTR, and sometimes the innermost NTR. This is displayed in the schematic figure below:

Figure 5.20: Schematic of the complex shaped NTR with both fixed and proportional costs.



Blue parallelogram stems from proportional costs, red ellipse stems from fixed costs. The purple dot is the placement of the Merton point, relative to the two NTRs at $t = T - 1$, known to be at the upper rightmost corner. The green dot is the placement of the Merton point, relative to the two NTRs at $t < T - 1$.

This NTR requires solutions of each separate NTR, the parallelogram and the ellipse that is, and then forming a convex hull as the outermost combination of these. The Angle of the fixe cost NTR and the proportional cost NTR stem from the correlation, so they are at least identical. However the proportional cost NTR could have no vertices outside the fixed cost NTR. Maybe it could have just two vertices outside the fixed cost NTR, or all the vertices could be outside the fixed cost NTR.

I consider this to be beyond the scope of this thesis, and do not consider this further, leaving this to future research in the field of dynamic portfolio choice with transaction costs.

6 Discussion

The dynamic portfolio choice problem with fixed or proportional costs has been introduced and solved in the previous sections. The framework developed in this thesis, is able to solve the problem that has been introduced in detail as well. I will now discuss the results, and the applicability and scalability of the model, competing implementation methods and avenues of future research in order to highlight the limitations of the model, and suggest areas for further research.

6.1 Applicability of the model

The model developed in this thesis is applicable to the problem of dynamic portfolio choice, with consumption, when investors face proportional transaction costs. While the model is only able to solve a reduced investment universe, in the number of assets, the results give a greater understanding of how transaction costs affect the optimal portfolio choice. Investment towards the optimal allocation may in fact be more costly than the transaction costs themselves, and the model provides a framework for understanding this trade-off. This is well known, and has been studied in the litterature of computational finance and behavioural finance.

However, since the results are only applicable to a reduced investment universe, the results may not be directly applicable to real world applications and remain theoretical in nature. First of, the the model predicts optimal behavior given the distribution of the asset returns, which are only available for past returns, and the distribution of future returns may differ from the distribution of past returns. Hence, the model suffers from the same limitations as other models in the field of finance, in that it is based on historical data, in my case simulated data even, and may not be applicable to future data.

Furthermore, even for parameters with high costs, as seen in prior sections, the simulation results showcase that only a miniscule amount of the wealth is lost due to fixed transaction costs.

For investors with a high wealth level, a pure fixed cost would be minuscule compared to the wealth level, and the resulting NTR would probably only be constructed from the proportional costs of which the implications were covered in Section 5.8.

Fixed cost NTRs are therefore mostly relevant for investors with a low wealth level, or investors who rebalance frequently, maybe multiple times a day. For these investors, the fixed cost is either relatively large, or incurred often.

For large institutional investors, the proportional cost NTR can still be relevant, as the proportional costs scale with the traded amount.

Until models with a large amount of assets, based on realistic distributional parame-

ters²⁰ are available, the model will mostly be relevant in a theoretical setting, or to give a general understanding of how transaction costs affect the optimal portfolio choice.

6.2 Scalability of the model

This thesis implements the framework constructed by (Gaegauf, Scheidegger and Trojani 2023) in order to solve the problem of dynamic portfolio choice with consumption, when investors face proportional transaction costs. This framework increases the scalability of the model to higher dimensions than previously possible without the use of super computers, by minimizing the number of grid points needed to approximate the NTR. However, the model is still computationally demanding, especially when the number of assets is high, and the number of grid points needed to train the function approximators still increase with the dimensionality of the model.

Furthermore, the evaluation of the increasingly complex GP increases exponentially in complexity with the number of assets. Also, even for the most simple shape of the NTR such as square, the number of vertices needed to effectively formulate the NTR increases exponentially with the number of assets. The framework is therefore not scalable to an arbitrary number of assets, and the number of assets that can be included in the model is limited by the computational power available. This limits the use of the model in real world applications, where the number of assets considered is high. Furthermore, distributional parameters would need to be estimated for each asset, which would further increase the computational complexity of a real world application.

For fixed costs a novel algorithm, based on the work of (Gaegauf, Scheidegger and Trojani 2023), and the geometric properties of the resulting NTRs is developed. The algorithm is able to solve the problem, but introduces a new set of challenges. While fewer initial points are needed, since I only need to approximate the center of the NTR in the first case, the bisection algorithm, needed to find the edge of the NTR, is computationally demanding, and re-introduces the need for evaluation at a fine grid along the trajectory from the center. Thus the fixed cost model poses further dimensional burden to the model. Furthermore, the edge points needed to approximate the NTR scale with dimensionality, when assets are correlated, as the resulting NTR is an ellipsoid. This, in combination with the bisection algorithm introduces curse of dimensionality to the model. Overall, a solution which can scale to a sufficiently large dimensionality, and which can be used in real world applications, is still yet to be found. However, this paper does provide a step in the right direction, by providing a framework which can be used to solve the problem in a higher dimensionality than previously possible, for the fixed cost case, which had previously not been solved for dimensions larger than two in a dynamic setting.

²⁰Which could stem from regressions on prior returns.

6.3 Competing implementation methods

As noted in the prior section. The frameworks used and developed in this paper, face scalability issues. Specifically the bisection algorithm used to find the edge of the NTR in the fixed cost case and the evaluation of the GP in the proportional cost case.

For the function approximators competing methods such as neural networks and other machine learning methods could be used to approximate the NTR. Neural networks are universal function approximators (Cybenko 1989), and could potentially approximate the NTR more efficiently than the GP. Since the goal is to approximate the NTR, if a neural network could be implemented to approximate the NTR more efficiently than the GP by skipping the evaluation of grid points necessary for the GP the model could scale better.

The bisection algorithm used to find the edge of the NTR in the fixed cost case, could likewise potentially be replaced by a more efficient algorithm. The bisection algorithm is favoured in this paper for its simplicity, and the fact that it is guaranteed to find the edge of the NTR. The algorithm is easy to understand in an intuitive manner, especially when the NTR is presented geometrically. The bisection algorithm could potentially be replaced by a root-finding algorithm leveraging the computed gradients in the current framework. Such a solver should theoretically be able to find the edge of the NTR more efficiently than the bisection algorithm, which needs to solve the model at each bisection mid point.

6.4 Avenues of Future Research

This thesis provides a framework for solving the problem of dynamic portfolio choice under various transaction costs and return structures. By first solving the problem over a fine grid, I find the geometric shape of the resulting NTR and then leverage this information to solve the problem more efficiently. This framework can be extended to various types of transaction costs. Notably (Dybvig and Pezzo 2020) consider asset specific fixed costs and price impact among other transaction costs not considered in this thesis. Future research could therefore consider other transaction cost structures, and combinations thereof, and how these affect the optimal portfolio choice, by using the proposed framework.

Furthermore, the framework could be extended to consider other asset structures. For example (Cai, Judd and Xu 2020) extend the model to include options on the assets considered in the model. (Dybvig and Pezzo 2020) consider hedging with futures, albeit still in a static setting. Futher research could consider how these asset structures affect the optimal portfolio choice, and how the framework can be extended to include these asset structures, which if still computationally feasible, would be a novel contribution to the literature, as the case of futures has not been tackled in a dynamic setting, and the case of options is computationally burdensome under the scheme of (Cai, Judd and Xu 2020). An analysis of price impact would likewise be interesting, specifically for large

institutional investors, whose trades can move the market and thus affect the price of the assets they are trading. The impact on the NTR in a dynamic setting would be interesting to see. The consumption model could also be extended to include other types of goods, such as durable consumption goods and how these affect the optimal portfolio choice.

7 Conclusion

The purpose of this thesis was to solve dynamic portfolio choice problems with proportional and fixed transaction costs and correlated return structures. In this regard, I constructed a new solution method, based on the work of (Gaegauf, Scheidegger and Trojani 2023).

My framework solved the problem, with fixed costs relative to wealth for more than two assets, which had not been done before to my knowledge, and provided a novel approach to the fixed cost problem. The framework builds on the geometric properties of the NTR, and combines the efficient solution method of (Gaegauf, Scheidegger and Trojani 2023) to solve the problem. I verified speculations on the geometric form of the fixed cost NTR, and the implications of correlated return structures on this type NTR. I find that the NTR with fixed costs and no correlation is sphere and not an ellipsoid. The NTR for fixed costs with correlations is a ellipsoid, with angle and size of major and minor axis, linked to the correlation structure. I conducted a simulation study, which showed that a strategy which takes costs into account, can outperform a strategy which does not. Lastly, I solved the model for a combination of fixed and proportional costs crudely, and found that the NTR is a combination of the two NTR.

Several limitations of the model remain, as discussed in Section 6. The model's applicability to real-world scenarios is constrained by its reliance on simulated data and reduced investment universes. While it provides theoretical insights, the assumptions about return distributions and the computational demands limit its use for large-scale, real-world portfolios. Additionally, the fixed-cost NTR is most relevant for small investors or frequent traders, whereas proportional costs remain more applicable to other investors.

I made four contributions along the way, which could prove useful for future research. First, I provided a novel approach to the fixed cost problem, based on the state of the art framework for proportional costs, which leverages the geometric shape of the NTR. Second, I solved dynamic portfolio choice problems with fixed costs for correlated assets, with more than two risky assets. Third, I presented findings on the combination of fixed and proportional costs and the resulting NTR shape in relation to the two costs. Fourth, I presented an approach to solving new transaction cost structures, not yet considered, and how to adapt my computational approach to these.

References

- Abrams, Robert A. and Karmarkar, Uday S. (1980). “Optimal Multiperiod Investment-Consumption Policies”. In: *Econometrica* Vol. 48, No. 2, pp. 333–353. ISSN: 00129682, 14680262.
- Akian, Marianne, Menaldi, José Luis and Sulem, Agnès (1996). “On an Investment-Consumption Model with Transaction Costs”. In: *SIAM Journal on Control and Optimization* Vol. 34, No. 1, pp. 329–364. DOI: 10.1137/S0363012993247159.
- Altarovici, Albert, Muhle-Karbe, Johannes and Soner, Halil Mete (2015). “Asymptotics for fixed transaction costs”. In: *Finance and Stochastics* Vol. 19, No. 2, pp. 363–414.
- Bellman, Richard (1958). “Dynamic programming and stochastic control processes”. In: *Information and Control* Vol. 1, No. 3, pp. 228–239. ISSN: 0019-9958. DOI: [https://doi.org/10.1016/S0019-9958\(58\)80003-0](https://doi.org/10.1016/S0019-9958(58)80003-0).
- Bertoni, Bridget (2010). “Multi-dimensional ellipsoidal fitting”. In: *Department of Physics, South Methodist University, Tech. Rep. SMU-HEP-10-14*.
- Björk, Tomas (2019). *Arbitrage theory in continuous time*. 4. ed. Oxford Univ. Press. ISBN: 9780198851615.
- Bono, Luca Maria Del, Nicoletti, Flavio and Ricci-Tersenghi, Federico (2024). *The most uniform distribution of points on the sphere*. arXiv: 2407.01503 [cond-mat.stat-mech].
- Cai, Yongyang, Judd, Kenneth L. and Xu, Rong (2013). *Numerical Solution of Dynamic Portfolio Optimization with Transaction Costs*. Working Paper 18709. National Bureau of Economic Research. DOI: 10.3386/w18709.
- Cai, Yongyang, Judd, Kenneth L. and Xu, Rong (2020). *Numerical Solution of Dynamic Portfolio Optimization with Transaction Costs*. Tech. rep. arXiv: 2003.01809 [q-fin.PM].
- Constantinides, George M. (1976). “Note—Optimal Portfolio Revision with Proportional Transaction Costs: Extension to Hara Utility Functions and Exogenous Deterministic Income”. In: *Management Science* Vol. 22, No. 8, pp. 921–923.
- Constantinides, George M. (1986). “Capital Market Equilibrium with Transaction Costs”. In: *Journal of Political Economy* Vol. 94, No. 4, pp. 842–862. ISSN: 00223808, 1537534X.
- Cybenko, George (1989). “Approximation by superpositions of a sigmoidal function”. In: *Mathematics of control, signals and systems* Vol. 2, No. 4, pp. 303–314.
- Davis, M. H. A. and Norman, A. R. (1990). “Portfolio Selection with Transaction Costs”. In: *Mathematics of Operations Research* Vol. 15, No. 4, pp. 676–713. DOI: 10.1287/moor.15.4.676.
- Dybvig, Philip H and Pezzo, Luca (2020). “Mean-variance portfolio rebalancing with transaction costs”. In: *Available at SSRN 3373329*.

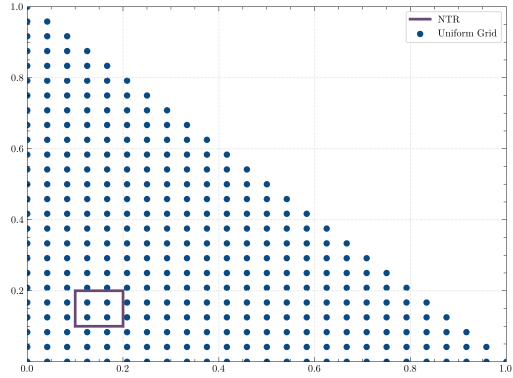
- Gaegauf, Luca, Scheidegger, Simon and Trojani, Fabio (2023). *A Comprehensive Machine Learning Framework for Dynamic Portfolio Choice With Transaction Costs*. Tech. rep. 23-114. Swiss Finance Institute, p. 70.
- Gander, Walter, Golub, Gene H and Strelbel, Rolf (1994). “Least-squares fitting of circles and ellipses”. In: *BIT Numerical Mathematics* Vol. 34, pp. 558–578.
- Glasserman, Paul (2004). *Monte Carlo methods in financial engineering*. New York, NY, USA: Springer. ISBN: 0387004513 9780387004518.
- Gonzalvez, Joan et al. (2019). *Financial Applications of Gaussian Processes and Bayesian Optimization*. Working Paper WP-80-2019. Document for the exclusive attention of professional clients, investment services providers and any other professional of the financial industry. Amundi Quantitative Research.
- Hok, J. and Kucherenko, S. (2023). *The importance of being scrambled: supercharged Quasi Monte Carlo*. arXiv: 2210.16548 [q-fin.CP].
- Horneff, Vanya, Maurer, Raimond and Schober, Peter (2016). “Efficient parallel solution methods for dynamic portfolio choice models in discrete time”. In: Available at SSRN 2665031.
- Ivanov, A. B. (2020). “Ellipse”. In: *Encyclopedia of Mathematics*. Adapted from the original article in the Encyclopedia of Mathematics - ISBN 1402006098. URL: <http://encyclopediaofmath.org/index.php?title=Ellipse&oldid=25305>.
- Janeček, Karel and Shreve, Steven E. (2004). “Asymptotic analysis for optimal investment and consumption with transaction costs”. In: *Finance and Stochastics* Vol. 8, No. 2, pp. 181–206. DOI: 10.1007/s00780-003-0113-4.
- Judd, Kenneth L. (1998). *Numerical Methods in Economics*. Vol. 1. MIT Press Books 0262100711. The MIT Press. ISBN: ARRAY(0x5a5be060). URL: <https://ideas.repec.org/b/mtp/titles/0262100711.html>.
- Judd, Kenneth L et al. (2014). “Smolyak method for solving dynamic economic models: Lagrange interpolation, anisotropic grid and adaptive domain”. In: *Journal of Economic Dynamics and Control* Vol. 44, pp. 92–123.
- Lesmond, David A., Ogden, Joseph P. and Trzezinka, Charles A. (1999). “A New Estimate of Transaction Costs”. In: *The Review of Financial Studies* Vol. 12, No. 5, pp. 1113–1141. ISSN: 08939454, 14657368.
- Liu, Hong (2004). “Optimal Consumption and Investment with Transaction Costs and Multiple Risky Assets”. In: *The Journal of Finance* Vol. 59, No. 1, pp. 289–338. ISSN: 00221082, 15406261.
- Markowitz, Harry (1952). “Portfolio Selection”. In: *The Journal of Finance* Vol. 7, No. 1, pp. 77–91. ISSN: 00221082, 15406261.
- Merton, Robert C. (1969). “Lifetime Portfolio Selection under Uncertainty: The Continuous-Time Case”. In: *The Review of Economics and Statistics*, pp. 247–257.

- Merton, Robert C. (1971). "Optimum Consumption and Portfolio Rules in a Continuous-Time Model". In: *Journal of Economic Theory* Vol. 3, No. 4, pp. 373–413. DOI: 10.1016/0022-0531(71)90038-X.
- Morton, Andrew J and Pliska, Stanley R (1995). "Optimal portfolio management with fixed transaction costs". In: *Mathematical Finance* Vol. 5, No. 4, pp. 337–356.
- Murphy, Kevin P. (2023). *Probabilistic Machine Learning: Advanced Topics*. MIT Press. URL: <http://probml.github.io/book2>.
- Muthuraman, Kumar and Kumar, Sunil (2006). "Multidimensional Portfolio Optimization with Proportional Transaction Costs". In: *Mathematical Finance: An International Journal of Mathematics, Statistics and Financial Economics* Vol. 16, No. 2, pp. 301–335.
- Muthuraman, Kumar and Kumar, Sunil (2008). "Solving Free-boundary Problems with Applications in Finance". In: *Foundations and Trends® in Stochastic Systems* Vol. 1, No. 4, pp. 259–341. DOI: 10.1561/0900000006.
- Oksendal, Bernt and Sulem, Agnès (2002). "Optimal Consumption and Portfolio with Both Fixed and Proportional Transaction Costs". In: *SIAM Journal on Control and Optimization* Vol. 40, No. 6, pp. 1765–1790. DOI: 10.1137/S0363012900376013.
- Pleiss, Geoff et al. (2018). *Constant-Time Predictive Distributions for Gaussian Processes*. arXiv: 1803.06058 [cs.LG]. URL: <https://arxiv.org/abs/1803.06058>.
- Schober, Peter, Valentin, Johannes and Pflüger, Dirk (2022). "Solving High-Dimensional Dynamic Portfolio Choice Models with Hierarchical B-Splines on Sparse Grids". In: *Computational Economics* Vol. 59, No. 1, pp. 185–224. DOI: 10.1007/s10614-021-10118-9.
- Shreve, S. E. and Soner, H. M. (1994). "Optimal Investment and Consumption with Transaction Costs". In: *The Annals of Applied Probability* Vol. 4, No. 3, pp. 609–692. DOI: 10.1214/aoap/1177004966.
- Smolyak, S. A. (1963). "Quadrature and Interpolation Formulas for Tensor Products of Certain Classes of Functions". In: *Doklady Akademii Nauk SSSR* Vol. 148. English translation: *Soviet Mathematics Doklady*, Vol. 4, pp. 240–243, pp. 1042–1043.
- Zabel, Edward (1973). "Consumer Choice, Portfolio Decisions, and Transaction Costs". In: *Econometrica* Vol. 41, No. 2, pp. 321–335.

Appendices

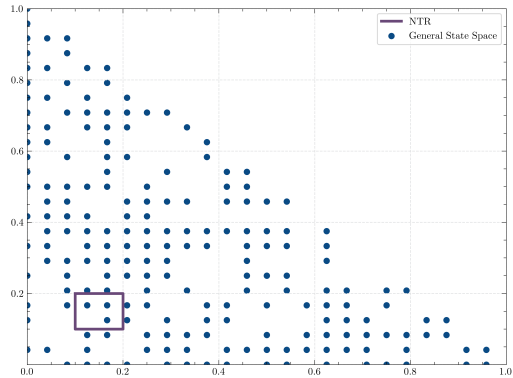
A Other sampling strategies

Figure A.1: Uniform grid sampling strategy



Note: Sample consists of $N = 200$ points.

Figure A.2: Naive random sampling strategy



Note: Sample consists of $N = 200$ points.

B No-Trade Region

No-Trade Region for $T - 1$:

$$\begin{bmatrix} 0.017 & 0.016 & 0.029 & 0.039 \\ 0.056 & 0.010 & 0.028 & 0.039 \\ 0.010 & 0.050 & 0.024 & 0.033 \\ 0.015 & 0.011 & 0.056 & 0.033 \\ 0.017 & 0.010 & 0.023 & 0.062 \\ 0.049 & 0.043 & 0.023 & 0.034 \\ 0.054 & 0.005 & 0.055 & 0.033 \\ 0.056 & 0.004 & 0.022 & 0.062 \\ 0.009 & 0.045 & 0.051 & 0.027 \\ 0.011 & 0.044 & 0.018 & 0.056 \\ 0.016 & 0.005 & 0.050 & 0.056 \\ 0.048 & 0.038 & 0.050 & 0.028 \\ 0.049 & 0.038 & 0.017 & 0.056 \\ 0.054 & 0.000 & 0.049 & 0.056 \\ 0.009 & 0.039 & 0.045 & 0.050 \\ 0.048 & 0.032 & 0.044 & 0.050 \end{bmatrix}$$

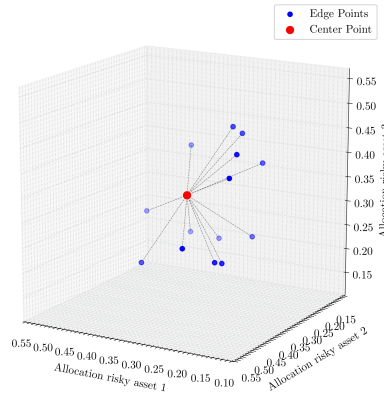
No-Trade region for $T - 2$:

$$\begin{bmatrix} 0.024 & 0.027 & 0.036 & 0.049 \\ 0.066 & 0.020 & 0.036 & 0.051 \\ 0.022 & 0.059 & 0.032 & 0.043 \\ 0.024 & 0.021 & 0.064 & 0.046 \\ 0.026 & 0.020 & 0.032 & 0.077 \\ 0.058 & 0.057 & 0.031 & 0.044 \\ 0.068 & 0.013 & 0.067 & 0.046 \\ 0.067 & 0.012 & 0.030 & 0.077 \\ 0.020 & 0.056 & 0.059 & 0.039 \\ 0.023 & 0.053 & 0.028 & 0.070 \\ 0.025 & 0.014 & 0.060 & 0.072 \\ 0.059 & 0.051 & 0.060 & 0.039 \\ 0.058 & 0.050 & 0.026 & 0.070 \\ 0.067 & 0.007 & 0.061 & 0.071 \\ 0.021 & 0.049 & 0.054 & 0.065 \\ 0.058 & 0.044 & 0.055 & 0.064 \end{bmatrix}$$

C Fitting the 3D fixed cost NTRs

Figure C.1: Fitting shceme for the 3D sphere NTR

Fitting the Circular NTR at time $t = T-1$



Fitting the sphere NTR with 3D data uses 14 points, more than necessary, to ensure a good fit